A Gently Processed Skim Milk-Derived Whey Protein Concentrate for Infant Formula: Effects on Gut Development and Immunity in Preterm Pigs

Aasmul-Olsen, Karoline; Akıllıoğlu, Halise Gül; Christiansen, Line Iadsatian; Engholm-Keller, Kasper; Brunse, Anders; Stefanova, Denitsa Vladimirova; Bjørnshave, Ann; Bechshøft, Mie Rostved; Skovgaard, Kerstin; Thymann, Thomas

Total number of authors:
13

Published in:
Molecular Nutrition and Food Research

Link to article, DOI:
10.1002/mnfr.202300458

Publication date:
2024

Document Version
Publisher's PDF, also known as Version of record

RESEARCH ARTICLE

Molecular Nutrition & Food Research
www.mnf-journal.com

A Gently Processed Skim Milk-Derived Whey Protein Concentrate for Infant Formula: Effects on Gut Development and Immunity in Preterm Pigs

*Karoline Aasmul-Olsen, Halise Gül Akıllıoğlu, Line Iadsatian Christiansen, Kasper Engholm-Keller, Anders Brunse, Denitsa Vladimirova Stefanova, Ann Bjørnshave, Mie Rostved Bechshøft, Kerstin Skovgaard, Thomas Thymann, Per Torp Sangild, Marianne Nissen Lund, and Stine Brandt Bering**

Scope: Processing of whey protein concentrate (WPC) for infant formulas may induce protein modifications with severe consequences for preterm newborn development. The study investigates how conventional WPC and a gently processed skim milk-derived WPC (SPC) affect gut and immune development after birth.

Methods and results: Newborn, preterm pigs used as a model of preterm infants were fed formula containing WPC, SPC, extra heat-treated SPC (HT-SPC), or stored HT-SPC (HTS-SPC) for 5 days. SPC contained no protein aggregates and more native lactoferrin, and despite higher Maillard reaction product (MRP) formation, the clinical response and most gut and immune parameters are similar to WPC pigs. SPC feeding negatively impacts intestinal MRP accumulation, mucosa, and bacterial diversity. In contrast, circulating T-cells are decreased and oxidative stress- and inflammation-related genes are upregulated in WPC pigs. Protein aggregation and MRP formation increase in HTS-SPC, leading to reduced antibacterial activity, lactase/maltase ratio, circulating neutrophils, and cytotoxic T-cells besides increased gut MRP accumulation and expression of *TNFAIP3*.

Conclusion: The gently processed SPC has more native protein, but higher MRP levels than WPC, resulting in similar tolerability but subclinical adverse gut effects in preterm pigs. Additional heat treatment and storage further induce MRP formation, gut inflammation, and intestinal mucosal damage.

1. Introduction

Human milk is the optimal diet for stimulating infant growth and development due to its nutritional composition and numerous bioactive components.[1,2] Feeding mother's own milk or donor human milk is, however, not always possible, which justifies the need for infant formulas (IFs). Although a considerable effort has been made to improve IFs, e.g., by increasing the amount of known bioactive milk components such as lactoferrin (LF),[3] human milk continues to be superior in reducing the risk of prematurity-associated complications following preterm birth.[4,5] Raw milk contains a wide variety of proteins and peptides, which apart from providing essential amino acids, encompass bioactive abilities such as antioxidant, antimicrobial, anti-inflammatory, and immune-stimulatory effects.[1,6–8] Thus, preserving the native state of bioactive milk components in bovine milk-based IF may be critical to simulate the functionality of mother's own milk. This

K. Aasmul-Olsen, L. I. Christiansen, A. Brunse, T. Thymann, P. T. Sangild, S. B. Bering
Section for Comparative Paediatrics and Nutrition
Department of Veterinary and Animal Sciences
University of Copenhagen
Frederiksberg 1870, Denmark
E-mail: sbb@sund.ku.dk

The ORCID identification number(s) for the author(s) of this article can be found under https://doi.org/10.1002/mnfr.202300458

DOI: 10.1002/mnfr.202300458

H. G. Akıllıoğlu, K. Engholm-Keller, M. N. Lund
Section for Ingredient and Dairy Technology
Department of Food Science
University of Copenhagen
Frederiksberg 1958, Denmark

D. V. Stefanova
Section for Microbiology and Fermentation
Department of Food Science
University of Copenhagen
Frederiksberg 1958, Denmark

A. Bjørnshave, M. R. Bechshøft
Arla Foods Ingredients Group P/S
Viby J 8260, Denmark

especially applies to the heat-labile proteins and particularly the bioactive whey proteins, which are abundant in human milk during early lactation.[9–11] Today, whey protein concentrate (WPC), a by-product isolated during cheese manufacturing, is the most used protein source for IFs. The multiple heat treatments included in the processing of WPC, secure microbiological safety, and long shelf life, but at the same time this can induce protein denaturation and subsequent aggregation, which has known implications for protein digestibility, bioavailability, and bioactivity.[12–16] In addition, chemical protein modifications through oxidation and Maillard reaction have favorable conditions during the processing and storage of milk.[14,17–20] In rodent models, gastrointestinal exposure to Maillard reaction products (MRPs) such as advanced glycation end products (AGEs) has been shown to elicit an inflammatory response upon binding to the receptor for AGEs (RAGE), which is present in healthy intestinal tissue.[21–23] Recently, we demonstrated that ultra-high temperature-treated ready-to-feed liquid IF increases the levels of MRPs during suboptimal storage, which induce gut inflammation when fed to preterm piglets.[24] Taken together, the formation of protein modifications during industrial processing and heat treatment of IF may partly explain the impaired gastrointestinal outcomes observed in piglets fed processed IF compared with intact bovine milk.[25–27] Hence, alternative gentle processing methods for whey protein ingredients to secure better gut and immune development during early life are needed. Using microfiltration techniques, whey protein concentrate can be produced directly from pasteurized skim milk (SPC). Multiple processing steps are thus avoided compared to the conventional WPC[28] and this has shown to preserve native protein structures.[29] The clinical effects of these changes to whey proteins in IFs when fed to sensitive newborns, e.g., those born preterm, are yet to be elucidated. On this background, we hypothesized that a gently processed SPC with retained bioactivity can improve intestinal maturation and immunity in IF-fed newborns and tested this in preterm newborn pigs relative to a conventional WPC. We further sought to document the effects of additional heat treatment and storage of SPC on structural protein modifications and MRP formation and putative clinical outcomes in pigs.

K. Skovgaard
Section for Protein Science and Biotherapeutics
Department of Biotechnology and Biomedicine
Technical University of Denmark
Lyngby 2800, Denmark
P. T. Sangild
Department of Pediatrics and Adolescent Medicine
Rigshospitalet
Copenhagen 2100, Denmark
P. T. Sangild
Hans Christian Andersen Children's Hospital
Odense 5000, Denmark
M. N. Lund
Department of Biomedical Sciences
Faculty of Health and Medical Sciences
University of Copenhagen
Copenhagen 2200, Denmark

2. Experimental Section

2.1. Preparation of Whey Protein Ingredients

All whey protein ingredients were produced by Arla Foods Ingredients Group P/S (Viby J, Denmark) and the process flow diagram is shown in **Figure 1**. The gently processed SPC powder ingredient was manufactured by fractionation of pasteurized bovine skim milk (72 °C, 15 s) using differently sized semipermeable membranes to reduce the lactose content, remove caseins, and increase the protein content on a dry matter basis, before spray drying using standard drying conditions (SPC). An additional heat treatment (80 °C, 30 s), mimicking pasteurization, was included before spray drying for the production of the heat-treated SPC ingredient (HT-SPC). A fraction of the HT-SPC powder ingredient was subsequently stored for 6 weeks at 37 °C, 70% relative humidity (HTS-SPC) to simulate extreme, yet authentic conditions, representing those in climatic zone IV.[30] The WPC powder ingredient was produced from pasteurized sweet whey, a by-product from cheese processing, using a conventional manufacturing method including ultrafiltration, diafiltration, and spray drying under standard drying conditions (WPC). The gross composition of the whey protein ingredients, as shown in **Table 1**, was analyzed using standard methods[31] and the final powders were kept at −80 °C until use.

2.2. Structural and Chemical Analysis of Whey Protein Ingredients

Color measurements were performed as previously described[32] and the browning index was calculated using values of lightness, redness, and yellowness.[33,34] The presence of disulfide-linked aggregates and nonreducible cross-links in the whey protein ingredients was analyzed by sodium dodecyl sulfate polyacrylamide gel electrophoresis (SDS-PAGE) under nonreducing and reducing (addition of dithiothreitol) conditions.[31] Polyacrylamide gels (NuPAGE Novex 12% Bis-Tris Gels, Invitrogen, Thermo Fischer Scientific, Waltham, MA, USA) were loaded with 20 µg protein per well. The intrinsic fluorescence emission spectra of the four ingredients were determined as previously described[35] with slight modifications. Briefly, samples were dissolved in 10 mM phosphate buffer (pH 7.0) at a concentration of 3% w/v by gentle stirring overnight in order to allow hydration and the pH was subsequently adjusted to 7.0. Prior to analysis, concentrations were adjusted to 0.05% w/v and the samples (150 µL) were then transferred to a 96-well microplate. The emission spectra (320–440 nm) were recorded using a SpectraMax i3x Multi–Mode Plate Reader (Molecular Devices, Sunnyvale, CA, USA) at 25 °C with an excitation wavelength of 295 nm (n = 6). The bandwidth of excitation and emission was 9 and 15 nm, respectively.

Glycation compounds (Amadori compounds determined as furosine, carboxymethyl lysine [CML], carboxyethyl lysine [CEL], methylglyoxal-derived hydroimidazolone [MG-H], glyoxal-derived hydroimidazolone [GO-H], glyoxal lysine dimer [GOLD], methylglyoxal lysine dimer [MOLD]) as well as amino acid crosslinks (lysinoalanine [LAL] and lanthionine [LAN]) were analyzed and quantified by LC-MS/MS after hydrolysis of the samples with 6 M HCl as previously described.[36] Hydrolysis was

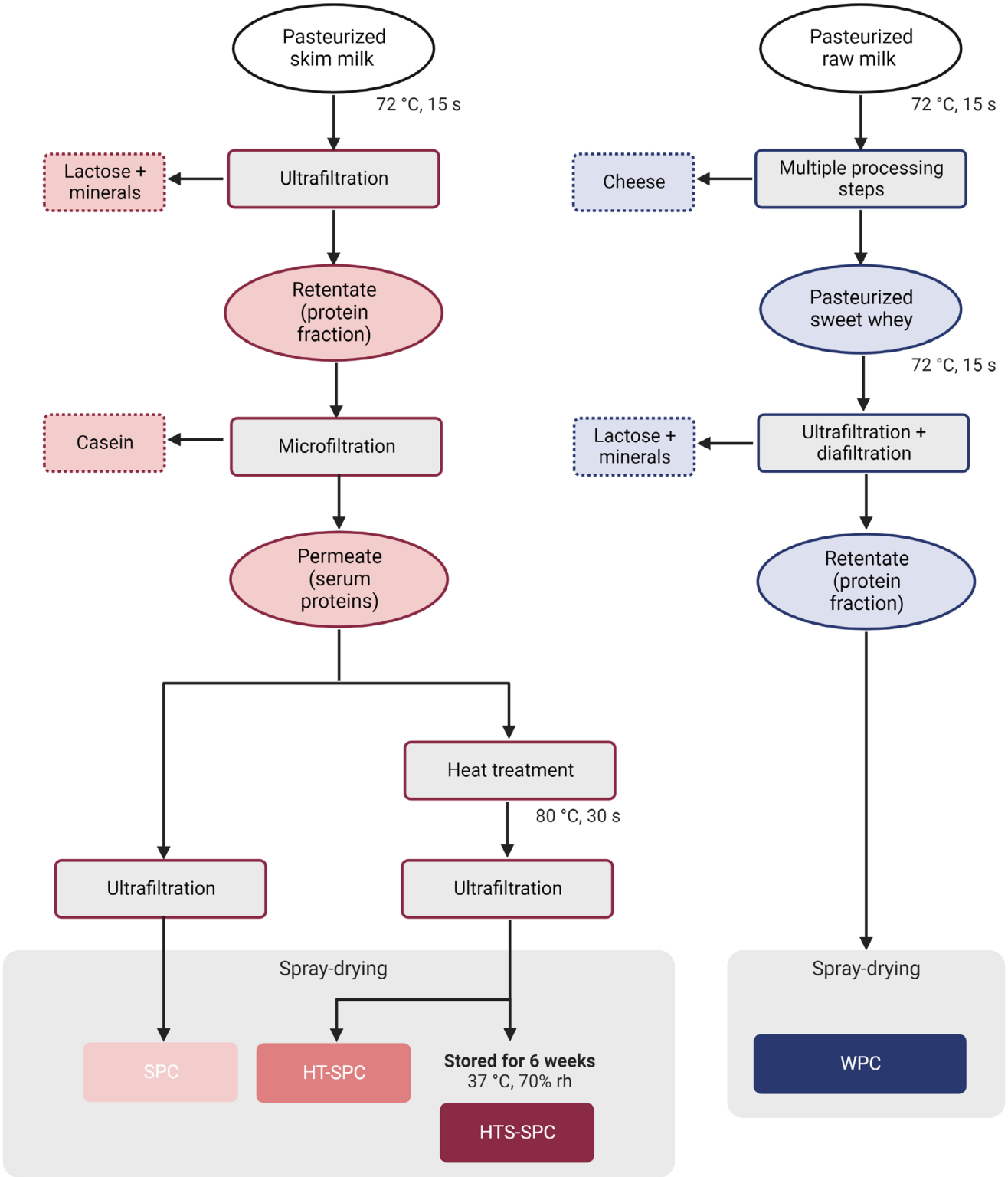

Figure 1. Process flow diagram for whey protein ingredients. Outline created in Biorender.com. HT-SPC, extra heat-treated (80 °C, 30 s) skim milk-derived whey protein concentrate; HTS-SPC, extra heat-treated (80 °C, 30 s) and stored (37 °C, 70% relative humidity, 6 weeks) skim milk-derived whey protein concentrate; SPC, skim milk-derived whey protein concentrate; WPC, conventional whey protein concentrate.

Table 1. Gross composition of whey protein ingredients (% w/w).

Whey protein ingredient	Dry matter [%]	Fat [%]	Protein [%]	Lactose [%]	Lactose/ Protein
WPC	94.7	5.68	77.7	7.46	0.10
SPC	95.9	0.25	78.8	10.6	0.13
HT-SPC	95.6	0.20	75.6	13.2	0.18
HTS-SPC	95.6	0.20	75.6	13.2	0.18

HT-SPC, extra heat-treated (80 °C, 30 s) skim milk-derived whey protein concentrate; HTS-SPC, extra heat-treated (80 °C, 30 s) and stored (37 °C, 70% relative humidity, 6 weeks) skim milk-derived whey protein concentrate; SPC, skim milk-derived whey protein concentrate; WPC, conventional whey protein concentrate.

performed in triplicate for each sample ($n = 3$) by microwave heating at 150 °C for 1 min followed by 10 min at 165 °C using a Biotage Initiator + microwave synthesizer (Biotage, Uppsala, Sweden). An additional reduction step with sodium borohydride was applied before hydrolysis of the samples for detection of CML.[36] The nonreduced hydrolysates were also used to analyze total amino acids. Free amino acids were extracted in two-steps. A total of 0.5 g sample was mixed with 5 mL water by vortexing, then centrifuged at 7500 × *g* for 10 min, after which the supernatant was collected. The pellet was washed with 2.5 mL water, centrifuged again, and the supernatant was pooled with the previously collected supernatant. Subsequently, 200 µL supernatant was mixed with 800 µL ice-cold methanol to precipitate the residual proteins (incubated at −80 °C for 1 h). Concentrations of free amino acids and protein-bound amino acid residues in the protein ingredients were calculated based on an external calibration curve using a standard mixture of amino acids containing Ala, Asp, Cys-Cys, Glu, Gly, His, Hyp, Ile, Leu, Lys, Met, Phe, Pro, Ser, Thr, Trp, Tyr, and Val as described previously.[37,38] The amino acid analysis was performed on a UHPLC-FLD instrument (Thermo Ultimate 3000 RS, Thermo Fischer Scientific) equipped with an Agilent AdvanceBio AAA column (100 × 3.0 mm, 2.7 µm, Agilent Technologies, Santa Clara, CA, USA). Analysis of α-dicarbonyl compounds was performed according to Akıllıoğlu et al.[39] Briefly, samples were dissolved in 50 mM phosphate buffer (pH 7.0) with gentle stirring overnight. Aliquots of 500 µL of sample solution was mixed with 1000 µL ice-cold methanol and incubated at –20 °C overnight. The samples were afterwards centrifuged at 22 000 × *g* for 15 min at 0 °C. The supernatant (500 µL) was mixed with 150 µL phosphate buffer (0.5 M, pH 7.0) and 150 µL OPD solution (0.2%, w/v) containing 18.5 mM diethylenetriaminepentaacetic acid. The samples were filtered immediately through 0.22 µm filters into UHPLC vials and incubated at 37 °C for 2 h in the dark for derivatization of the α-dicarbonyl compounds. The quinoxaline derivatives of glucosone, galactosone, 3-deoxyglucosone (3-DG), 3-deoxygalactosone (3-DGal), 1-deoxyglucosone (1-DG), 3,4-dideoxyglucosone-3-ene (3,4-DGE), 3-deoxypentosone (3-DP), 1-deoxypentosone (1-DP), glyoxal, methylglyoxal, and dimethylglyoxal were analyzed by LC–MS. Chromatographic and mass spectrometric conditions were described previously.[39] Solutions of glyoxal, methylglyoxal, dimethylglyoxal, and glucosone in the range of 1–250 ng mL^{-1} were derivatized as outlined for the samples and analyzed to build the external calibration curve of their quinoxaline, 2-methylquinoxaline, 2,3-dimethylquinoxaline, and glucosone quinoxaline forms, respectively. Quantification of 3-deoxyglucosone was based on the 2-(2′, 3′, 4′-trihydroxybutyl) quinoxaline (quinoxaline form of 3-deoxyglucosone) standard prepared in the range of 2–250 ng mL^{-1}. Concentrations of galactosone were determined based on glucosone and 3-DGal, 1-DG, 3,4-DGE, 3-DP, 1-DP were quantified based on the standard curve of 3-DG, after confirming their identity with LC-MS. 5-hydroxymethylfurfural (HMF) analysis was performed as described in Akıllıoğlu et al.[39]

2.3. In Vitro Bioactivity of Whey Protein Ingredients

The LF concentration and in vitro antibacterial property of the protein ingredients were used to assess differences in bioactivity. For each sample, three technical replicates were prepared by resuspending 10 mg powder in 10 mL Milli-Q water (using a magnetic stirrer for 1 h at room temperature) before analyzing the samples using a commercial bovine LF ELISA kit according to the manufacturer's instructions (LSBio, Seattle, WA, USA). An LC-MS analysis was subsequently used to validate the ELISA results. Approximately 100 mg WPC, SPC, HT-SPC, and HTS-SPC powder, respectively, was dissolved in 1 mL of 8 M urea by brief vortexing followed by shaking for 30 min at 800 rpm on an IKA Vibrax VXR orbital shaker (IKA-Werke, Staufen, Germany). The solution was centrifuged for 10 min at 14 000 × *g* at 22 °C. The supernatant was then transferred to a 15 mL tube and 4 mL ice-cold acetone was added, followed by incubation for 1 h at −20 °C. The tube was centrifuged at 4500 × *g* for 15 min at 4 °C, the acetone was removed, and the tubes were left with the lid off to let residual solvent evaporate. The protein pellet was dissolved in 2 mL 8 M urea using vortexing, followed by aspiration and dispensing 20 times through an 18-gauge needle using a 5 mL plastic syringe. The samples were adjusted to a final concentration of 50 mM ammonium bicarbonate, 10 mM TCEP with 1 M ammonium bicarbonate solution, and 1 M TCEP stock solutions, respectively. 5 µL sample (250 µg protein) of each condition was mixed with 5 µL Lys-C (0.005 AU µL^{-1}) in 100 mM ammonium bicarbonate and incubated with mixing at 900 rpm, 25 °C for 3 h. 1.1 µL 200 mM iodoacetamide was added, and the samples were incubated with shaking at 800 rpm, 22 °C for 30 min. 20 µL 0.5 µg µL^{-1} TrypZean in 50 mM ammonium bicarbonate were then added, and the samples were incubated for 18 h with shaking at 800 rpm, 22 °C. The samples were analyzed using a Thermo Exploris 480 mass spectrometer equipped with a Thermo Vanquish Flex UHPLC system. Each sample (0.5 µL) was injected onto a Phenomenex Aeris C18 (150 × 2.1 mm 2.6 µm particle size) reversed phase column (at 40 °C) using an Ultimate 3000 UHPLC system (Thermo Fischer Scientific). Peptides were analyzed using an 18 min LC-MS/MS run at a flow rate of 250 µL min^{-1}, being eluted off the column using an increasing gradient of mobile phase A (0.1% formic acid) to B (90% acetonitrile, 0.1% formic acid) (0.0–2.0 min: 3% B; 2.0–3.0 min: 3–15% B; 3.0–12.0 min: 15–45% B; 12.0–13.0 min: 45–90% B; 13.0–14.0 min: 90% B; 14.0–15.0 min: 90–3% B; 15.0–18.0 min: 3% B). Eluted peptides were introduced into the mass spectrometer via an OptaMax NG heated electrospray source (Thermo Fischer Scientific) in positive ion mode with the following conditions: 3.5 kV spray voltage, sheath gas setting 50, aux gas setting 10, sweep gas setting 1, and vapor-

izer temperature of 350 °C. A full MS scan of the *m*/z 200–2000 range was acquired in the Orbitrap (full width at half maximum [FWHM] resolution of 60 000) with an AGC target of 1×10^6. For each full scan, the top 10 most intense ions with intensity higher than 5×10^4 (charge state 1+ to 8+) were selected for higher-energy collision dissociation (HCD) and detected at a resolution of 7500 FWHM. Settings for the HCD event were as follows: the maximum injection time mode was set to "auto" at the MS level and custom at the MS/MS level with a normalized AGC target of 1000%. The isolation window was 1.4 Da, first fixed mass was 140, normalized collision energy was 26, "peptide match" was off, "exclude isotopes" was on, and "dynamic exclusion" was in auto mode.

To identify the tryptic peptides from the LC-MS/MS raw data, peak list generation and database searching of the peak lists against a concatenated forward/reverse protein database were performed using the MaxQuant software version 1.5.8.3.[40] The protein database contained 100 milk proteins with the highest summed ion intensity obtained from a previous LC-MS/MS analysis of skim milk, plus common contaminants often observed in proteomic analyzes of biological samples (345 proteins in total). Default parameters were used except for the following: Enzyme was Trypsin/P, minimum peptide length was six. The following variable modifications were allowed: acetylation of protein N-termini, oxidation (+16 Da) of Met, carboxymethylation (+58 Da) of Lys, Arg and protein N-termini, lactosylation (+324 Da) of Lys and protein N-termini, glycation (+162 Da) of Lys and protein N-termini, and deamidation of Gln and Asn (+1 Da). "Match between runs" was enabled with a matching time window of 0.7 min and an alignment time window of 10 min. Relative quantification based on the summed peptide peak apex intensities in MaxQuant was performed using peptides (both nonmodified and modified) unique to each individual protein in the database. Bovine LF (Uniprot accession number P24627) was identified based on 31 different peptide sequences, of which 27 peptides were unique to P24627.

The bacterial growth inhibitory capacity of the four resuspended protein ingredients (equivalent to the amounts used in the pig study) was tested against *Staphylococcus epidermidis* (inoculated at 10^5 and 10^6 CFU mL^{-1}) and *Enterococcus faecalis* (inoculated at 10^4 and 10^5 CFU mL^{-1}) as previously described.[24] *S. epidermidis* and *E. faecalis* were previously identified as the two most prevalent bacterial species isolated from the bone marrow of 5-day-old preterm piglets.[41,42] Bacterial growth after 2, 4, and 6 h of incubation at 37 °C with the WPC, SPC, HT-SPC, and HTS-SPC resuspension was determined in triplicates by CFU counts following dilution plating on blood agar.[43]

2.4. Animal Experimental Procedures

This study was designed and conducted in accordance with the EU directive 2010/63/EU for animal experiments under a license issued by the Danish Animal Experiments Inspectorate (license no.: 2014-15-0201-00418). Reporting of the animal experimental work comply with the ARRIVE guidelines 2.0.[44] In total, 72 preterm piglets (Landrace × Yorkshire × Duroc, male:female ratio 37:35) from three healthy commercially bred sows were successfully resuscitated upon delivery by caesarian section at approximately 90% gestation (full gestational length: 117 ± 2 d). The sample size was chosen based on a previous study demonstrating clear gut effects of a bioactive WPC in a lactose-dominant formula.[13] Immediately after birth, umbilical arterial catheters and orogastric feeding tubes were surgically placed for all piglets, enabling the provision of continuous parenteral and bolus-administered enteral nutrition, respectively.[45] Piglets were then stratified according to birth weight and sex into four groups, which were randomly assigned one of four dietary interventions with either SPC, HT-SPC, HTS-SPC, or WPC powder added to a standard lactose-based formula as the sole enteral protein source. The total enteral protein level, 70 g L^{-1} formula, was normalized to the protein content of the ingredients. The same amounts of lactose, medium- and long-chained fatty acids, minerals, and vitamins were added to the final formula diets (Table S1, Supporting Information), resulting in similar energy levels (3593–3723 kcal). Formula diets were stored at 4 °C after fresh blending every other day, and the required volumes were heated to 37 °C just before each bolus feeding (every 3 h). The enteral and parenteral nutrition, based on the Kabiven chamber bags for human use (Fresenius Kabi, Uppsala, Sweden), were both adjusted to support the requirements of piglets.[45] In accordance with the established preterm pig necrotizing enterocolitis (NEC) model,[45] enteral feeding was introduced from birth at 24 mL kg^{-1} d^{-1}, and increased gradually during the 5-day study to reach full enteral feeding from day 4, i.e., 100 mL kg^{-1} d^{-1}, while parenteral infusions simultaneously decreased (4.00–2.67 mL kg^{-1} h^{-1}). Piglets were housed individually in heated incubators with initial oxygen supply (1–2 L min^{-1} for 24 h) and controlled ventilation. In-cage physical activity was measured by continuous infrared video surveillance connected to a motion detection software (PigLWin, Ellegaard Systems, Faaborg, Denmark) as previously described.[46] During the first 24 h after birth, 16 mL kg^{-1} of maternal plasma was infused through the umbilical arterial catheters to assist the piglets' passive immunization.

2.5. Clinical Evaluation, Necropsy, and Tissue Collection

Body weights were recorded each morning while clinical (1–4, best to worst) and fecal scores (1–4, 4 = diarrhea) were assessed by experienced blinded personnel twice daily.[47] Animals were continuously monitored for clinical deterioration and humane endpoints (signs of NEC or systemic illness with no response to treatment) were defined before the study commenced. If reached, piglets were immediately euthanized. From day 4 onwards, as piglets received full enteral nutrition, tissue was collected according to the sample protocol described below. In individual cases of feeding intolerance the enteral bolus(es) were either halved or skipped. The assessment of feeding intolerance was based on gastric residuals, emesis, abdominal distension, and/or diarrhea. Intestinal absorptive capacity was measured on day 4 by the increment of plasma galactose 20 min after administration of an oral bolus of 15 mL kg^{-1} of a 5% galactose solution.[24]

On day 5, the piglets received a standardized last enteral bolus with 6 mg mL^{-1} Cr_2O_3 1 h prior to blood sampling via cardiac puncture and euthanasia, performed as previously described.[47] Following excision of abdominal organs, the passage length of

chromium oxide was measured, and the most distal gastrointestinal segment where the chromium oxide marker could be seen (stomach, proximal, middle, or distal small intestine, colon, or rectum) was recorded. Severity and distribution of gross pathological changes of the stomach, small intestinal regions, and colon were determined by two blinded investigators in accordance with an established six-grade NEC scoring system.[48] A score of ≥4 for any of the five gastrointestinal segments meant macroscopic lesions consistent with NEC. To evaluate small intestinal mucosal damage, and a candidate biomarker of NEC, the plasma intestinal fatty acid-binding protein (I-FABP) level was measured in pre-euthanasia blood samples using a human commercial ELISA kit (HycultBiotech, Uden, The Netherlands). Before gut tissue collection, internal organs were weighed, including the stomach content, for assessment of the gastric emptying rate. Tissues from the proximal, middle and distal small intestine were snap-frozen and cryopreserved for later measurements of, e.g., brush border enzyme activities.[49] Further, fixed transverse sections of the small intestine were embedded in paraffin, sectioned and stained with hematoxylin and eosin for later histological examination including villus/crypt measurements.[50] Tissue collected from the ascending colon was homogenized using M-tubes on a gentleMACS Dissociater (Miltenyi Biotec, Bergisch Gladbach, Germany) as previously described.[27] The level of proinflammatory cytokines (tumor necrosis factor (TNF-α), IL-Iβ, and IL-8) was measured in homogenate supernatants using porcine DuoSet ELISA kits according to the manufacturer's instructions (R&D Systems, Abingdon, UK). Finally, the left hind leg was released at the hip joint and a bone marrow biopsy was collected in a sterile way from the femur following a transection of the distal epiphysis. To assess bacterial accumulation and used as an indicator of bacterial gut translocation, the bone marrow biopsy was homogenized in sterile saline using a homogenizer (Stomacher 400, Seward, West Sussex, UK) and CFU g^{-1} bone marrow were counted based on dilution plating on blood agar after aerobic incubation overnight at 37 °C.

2.6. Glycation Products, Amino Acid Cross-Links and Gene Expression in the Small Intestine

Distal small intestinal tissue samples were freeze-dried and pulverized before each was divided into two fractions. One fraction was homogenized in NP40 cell lysis buffer (150 mM NaCl, 1% Triton X-100 and 50 mM Tris) using a gentle MACS Dissociator (Miltenyi Biotec) and the total protein content was subsequently determined by a bicinchoninic acid protein assay kit according to the manufacturer's instructions (Thermo Fisher Scientific). The second fraction was hydrolyzed with 6 M HCl prior to the analysis of glycation products and amino acid cross-links as described previously for protein ingredients.

For gene expression analysis, homogenization of the distal small intestinal tissue was performed using either RLT buffer (Qiagen, Hilden, Germany) or QIAzol Lysis Reagent (Qiagen), to ensure enough RNA extracts of sufficient quality. RNA extraction was achieved using the RNeasy Mini kit (Qiagen) including on-column DNase digestion (RNase-Free DNase Set, Qiagen) according to the manufacturer's specifications. RNA purity and quantity were determined using a NanoDrop 1000 spectrophotometer (Thermo Fischer Scientific) and RNA integrity was measured with an Agilent 2100 Bioanalyzer (Agilent Technologies) and appertaining Agilent RNA 6000 Nano kit (Agilent Technologies). In total, 29 samples (n = 7–8 per group) with a median (IQR) RNA integrity number of 5.3 (4.5–6) were used for subsequent microfluidic high-throughput real-time qPCR. The expression profiles of genes involved in gut maturation and inflammation, including AGE-RAGE downstream pathways, were measured using specific porcine primers (Table S2, Supporting Information). Briefly, three separate technical replicates of cDNA were synthesized from each RNA sample (500 ng total RNA) using a QuantiTect Reverse Transcription Kit (Qiagen) according to the manufacturer's specifications. Triplicates of samples were prepared to overcome issues related to the low RNA integrity and the primer assays selected have previously been found to be relatively tolerant to degraded RNA. Preamplification, using the TaqMan PreAmp Master Mix (Applied Biosystems, Waltham, MA, USA), and subsequent Exonuclease 1 (New England Biolabs, Ipswich, MA, USA) treatment was carried out as previously described.[51] Two 96.96 Dynamic Array Integrated Fluidic Circuit chips and the Biomark platform (Fluidigm, South San Francisco, CA, USA) were used for qPCR of the preamplified cDNA samples including nonreverse transcriptase controls and non-template controls.[51] Melting curves and Cq values were retrieved using the Fluidigm Real-Time PCR Analysis software (version 4.7.1, Fluidigm) and relative quantities were calculated after inter plate calibration, primer efficiency corrections and normalization to validated internal reference genes (*ACTB*, *GAPDH*, *HPRT1*, *PPIA*, and *YWHAE*, Table S2, Supporting Information) using the GenEx program (version 7, MultiD, Göteborg, Sweden). Data were log2-transformed prior to statistical analysis.

2.7. 16S rRNA Gene Amplicon Sequencing of Colon Content

DNA was extracted from 100 mg colon content per sample using Micro Bead beat AX kit (A&A Biotechnology, Gdańsk, Poland). 16S rRNA gene amplicon sequencing was performed using the GridIONX5 platform (Oxford Nanopore Technologies, Oxford, UK) as previously described.[52] A barcoded sequencing library was prepared with a two-step PCR targeting V1–V9 regions of the bacterial 16S rRNA gene, using multiple primer sets including unique molecular identifier sequences. PCR products were purified using AMPure XP beads (Beckman Coulter Genomic, CA, USA). All DNA amplicons were pooled at equimolar concentrations and subjected to 1D genomic DNA by ligation protocol (SQK-LSK114) to complete library preparation for GridIONX5 sequencing. Approximately 0.2 µg of amplicons were used for the initial step of end-prep, and 20 ng of library was loaded onto an R10.4.1 flow cell. Sequencing data were collected, base-called, trimmed, and demultiplexed as previously described.[52] Resulting fastq files were quality filtered using NanoFilt ($q \geq 10$; read length > 1Kb) and subsequently subjected to taxonomic assignment using SILVA, high-quality rRNA database version 138.1. Downstream analyzes were performed using the phyloseq package in R (version 4.2.3, R Foundation for Statistical Computing, Vienna, Austria). Alpha diversity was expressed as Shannon index in data normalized to the mean read count. Beta diversity as a measure of bacterial community structure was computed

in Bray-Curtis dissimilarity metric after cumulative sum scaling normalization and analyzed by permutational multivariate analysis of variance. The differential abundance analysis was based on DESeq2, using an adjusted probability value of 0.05 (Wald test with Benjamin-Hochberg correction) and a minimum log2-fold change of ± 1.5, corresponding to a difference in relative abundance of ≈3. Figures were created using the ggplot2 package.

2.8. Profiling and Function of Systemic Immune Cells

Blood samples obtained on day 5 were subjected to routine hematological and biochemical analysis as described elsewhere.[47] Further, immune assays evaluating neutrophil phagocytosis, T-cell subsets, and the early immune response to an ex vivo stimulation with live bacteria were conducted. The BD Accuri C6 flow cytometer (BD Biosciences, Franklin Lakes, NJ, USA) was used for T-cell subset profiling and evaluating the phagocytic rate and activity of neutrophils as previously described.[53,54] Populations of T cells (CD3+ lymphocytes), helper T cells (T_H, CD3+CD4+CD8- lymphocytes), cytotoxic T cells (T_C, CD3+CD4-CD8+ lymphocytes), and regulatory T cells (T_{Reg}, CD3+CD4+FoxP3+ lymphocytes) were identified. For the immune competence assay, whole blood was inoculated with live *S. epidermidis* (2×10^6 CFU mL^{-1}) and incubated at 37 °C for 2 h together with unstimulated controls. Following centrifugation at 2000 × *g* for 10 min at 4 °C, the supernatant was collected and TNF-α levels determined before and after stimulation using the above-mentioned porcine DuoSet ELISA kit.

2.9. Statistics

For all endpoints, two separate statistical analyzes were performed in R, with the first comparing WPC to SPC and the second comparing the three SPC ingredients. Repeated measurements of continuous variables were analyzed using a linear mixed effects model (lme function) including the pig as a random effect for in vivo/ex vivo data (i.e., body weights, in-cage physical activity, gut parameters measured across the small intestine and results from the blood stimulation assay) and the experimental period as a random effect for in vitro data (i.e., results from the antibacterial assay). In addition, a Gaussian correlation structure was included in the model for body weights. Group comparisons at individual time points were facilitated by the lsmeans package. A multiple linear regression model (lm function) was applied for all other continuous data. Incidences of feeding intolerance, diarrhea, NEC, and bone marrow infection were evaluated by the generalized multiple linear regression model (glm) with a binomial response and logit link. NEC scores and the passage length of chromium oxide were analyzed by ordinal logistic regression (polr function). A cox proportional hazard model (coxph function) was used to evaluate the passage of meconium. Sex, litter, and birthweight were included as fixed effects in all the above-mentioned models concerning data from the pig study. To adjust for multiple comparisons, the Tukey's post hoc test was used when comparing SPC ingredients and the Holm correction was employed for blood biochemistry data. Graphical validation of the normality and homoscedasticity assumptions was performed for all linear regression models including data transformations (log or sqrt) if needed. The nonparametric Mann–Whitney and Kruskal–Wallis with Dunn's post hoc test were used if data could not be transformed when comparing two and three groups, respectively. The goodness-of-fit test (g of package) was used to evaluate the cumulated residuals and validate regression models with a binomial response variable. Raw data are presented as means ± SD, unless otherwise stated, and *p*-values < 0.05 were regarded as statistically significant.

3. Results

3.1. Protein Structure and Bioactivity of Whey Protein Ingredients

The amino acid compositional analysis revealed some differences between the WPC and SPC ingredients (Table S3, Supporting Information). Compared to SPC, we measured a higher level of threonine and a lower level of tyrosine (both $p < 0.05$), while the branched-chain amino acid isoleucine was more abundant and its isomer leucine less abundant in WPC (both $p < 0.01$). Due to the filtration processes, free amino acids were largely removed and their concentrations therefore below the limit of quantification. SDS-PAGE was performed to further examine compositional differences between the ingredients in addition to structural protein modifications. The greater intensity of the protein band at ≈14 and ≈18 kDa, observed in SPC, indicate a higher level of α-lactalbumin and β-lactoglobulin, respectively, compared to WPC. In contrast to SPC, a high-molecular-weight smear (>260 kDa) was observed under nonreduced conditions for WPC, HT-SPC, and HTS-SPC, indicating the presence of large aggregates in these ingredients (**Figure** 2A). As the smears almost disappeared after reduction with dithiothreitol, the aggregates were primarily disulfide-based cross-links. WPC could also be distinguished based on the intrinsic fluorescence emission spectra, which revealed a decrease in fluorescence intensity compared to the SPC ingredient (Figure 2B). Finally, we observed a peak shift towards a higher wavelength of HTS-SPC relative to SPC ($p < 0.05$).

The LF level in the whey protein ingredients was measured by LC-MS and ELISA to determine the total and native amounts, respectively. The total amount of LF in the various SPC ingredients was similar and approximately 2.5 times lower than in WPC ($p < 0.001$; Figure 2C). Contrary, ELISA results showed lower levels of native LF in WPC ($p < 0.05$), HT-SPC ($p < 0.001$), and HTS-SPC ($p < 0.001$) compared to SPC (Figure 2D). The antibacterial ability of the ingredients was evaluated against *S. epidermidis* and *E. faecalis*. For *S. epidermidis*, an inoculation dose of 10^6 CFU mL^{-1} provided the most sensitive assay, with WPC and SPC having a similar bacterial growth inhibitory capacity. At both 4 and 6 h of incubation with SPC, the bacterial growth curve was lower than that following incubation with HT-SPC and HTS-SPC ($p < 0.01$; Figure 2E). When the ingredients were inoculated with 10^5 CFU mL^{-1} *S. epidermidis*, similar but slightly lower bacterial growth curves were observed. For *E. faecalis* the bacterial growth curve was higher when incubated with WPC than SPC ($p < 0.05$; Figure 2E). This difference was already detected at 2 h of incubation and persisted throughout the incubation period for both inoculation dose 10^4 and 10^5 CFU mL^{-1}.

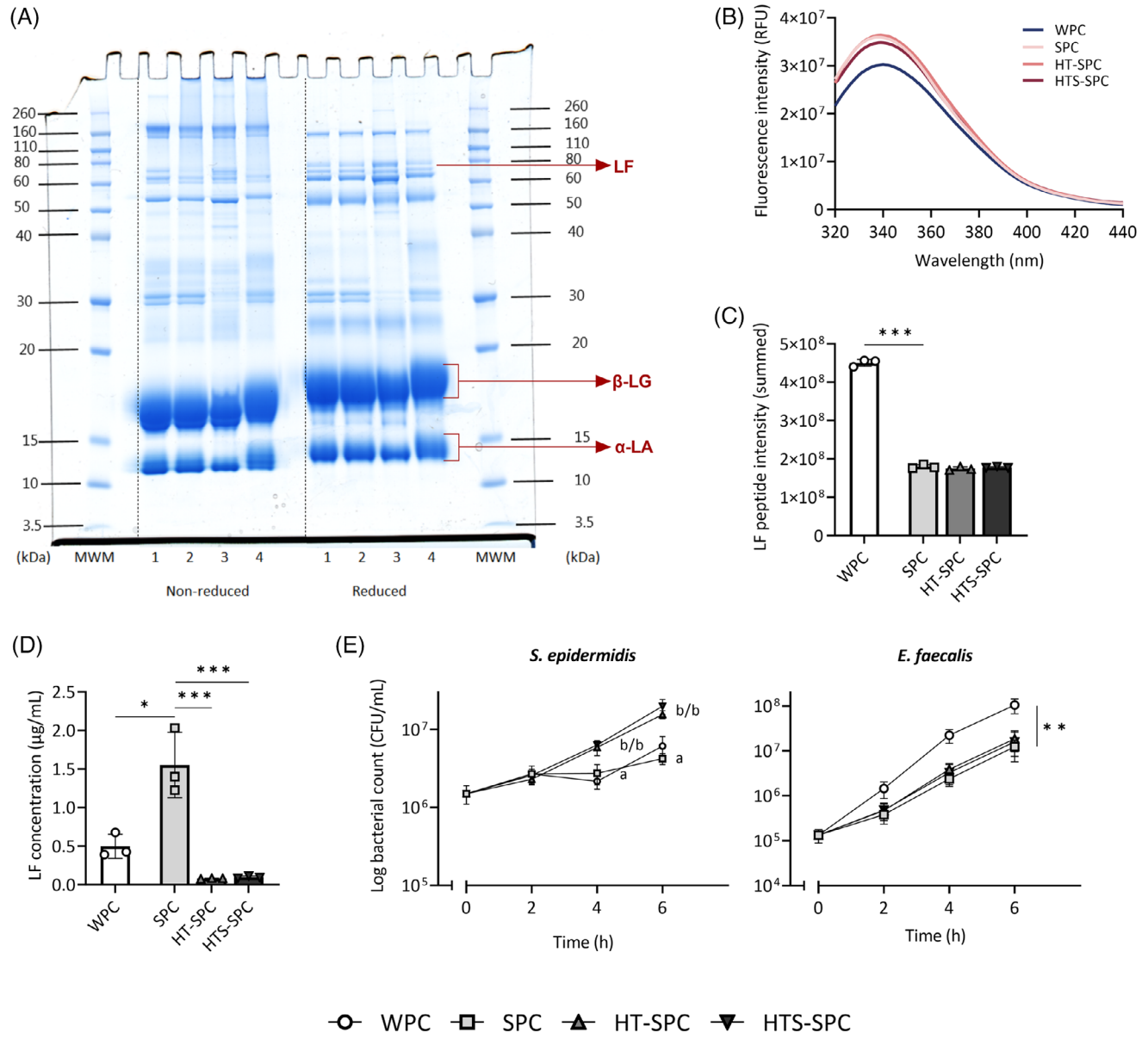

Figure 2. Structural protein modifications and bioactivity of whey protein ingredients. A) SDS-PAGE gel loaded with 20 µg protein per well of SPC (1), HT-SPC (2), WPC (3), and HTS-SPC (4) under non-reduced and reduced conditions. Dotted vertical lines represent cropped-out lanes containing excluded samples. B) Intrinsic fluorescence emission spectra; λ_{max} of WPC: 340 ± 0.6, SPC: 338 ± 0.9, HT-SPC: 339 ± 0.5, and HTS-SPC: 339 ± 0.8. C) Relative LF quantification in whey protein ingredients using peptide-based LC-MS analysis. D) LF level in whey protein ingredients measured by ELISA. E) Growth curves of *S. epidermidis* 10^6 CFU mL^{-1} (left panel) and *E. faecalis* 10^5 CFU mL^{-1} (right panel) following incubation with whey protein ingredients. Values (mean ± SD, n = 3–6 per group) not sharing the same letters are significantly different ($p < 0.001$). *, $p < 0.05$; **, $p < 0.01$; ***, $p < 0.001$. α-LA, α-lactalbumin; β-LG, β-lactoglobulin; HT-SPC, extra heat-treated (80 °C, 30 s) skim milk-derived whey protein concentrate; HTS-SPC, extra heat-treated (80 °C, 30 s) and stored (37 °C, 70% relative humidity, 6 weeks) skim milk-derived whey protein concentrate; MWM, molecular weight marker; SPC, skim milk-derived whey protein concentrate; WPC, conventional whey protein concentrate.

3.2. Effects of Heat Treatment and Storage on the Development of MRPs and Amino Acid Cross-Links in Whey Protein Ingredients

Color measurements revealed differences in browning index between the whey protein ingredients (WPC: 12.6 ± 0.2, SPC: 8.71 ± 0.04, HT-SPC: 8.51 ± 0.14, HTS-SPC: 10.1 ± 0.2). A more intense browning was measured in WPC compared to SPC ($p <$ 0.001), however, the color formation increased during storage of SPC, resulting in an enhanced browning index of HTS-SPC compared to SPC and HT-SPC (both $p < 0.001$). α-Dicarbonyl compounds and protein modifications in the form of glycation products and amino acid cross-links are given in **Table 2**. The 3-DGal was the most abundant α-dicarbonyl compound, and while a similar level was measured in SPC and HT-SPC, the concentration was higher in HTS-SPC (both $p < 0.001$). In general, six-carbon

Table 2. Maillard reaction products and amino acid-derived cross-links in whey protein ingredients.

Products	WPC	SPC	HT-SPC	HTS-SPC	p-value$_1$	p-value$_2$
α-Dicarbonyl compounds, μg g^{-1} sample						
Glyoxal	0.60 ± 0.12	2.29 ± 0.25^b	2.31 ± 0.35^b	<LOQ^a	<0.01	<0.001
Methylglyoxal	0.60 ± 0.01	1.36 ± 0.01^c	0.64 ± 0.05^b	0.24 ± 0.03^a	<0.001	<0.001
Dimethylglyoxal	2.00 ± 0.38	1.06 ± 0.40	1.06 ± 0.30	1.52 ± 0.15	0.168	0.502
3-DG	2.45 ± 0.05	2.91 ± 0.05^a	2.72 ± 0.04^a	3.27 ± 0.09^b	<0.01	<0.01
3-DGal	6.42 ± 0.14	4.66 ± 0.12^a	4.29 ± 0.13^a	6.36 ± 0.12^b	<0.001	<0.001
1-DG	2.40 ± 0.01	4.08 ± 0.08^a	4.18 ± 0.08^a	4.55 ± 0.04^b	<0.001	<0.01
3,4-DGE	3.36 ± 0.06	2.88 ± 0.04^b	2.58 ± 0.02^a	3.56 ± 0.03^c	<0.01	<0.001
3-DP	1.24 ± 0.01	1.39 ± 0.01^b	1.38 ± 0.03^b	1.20 ± 0.02^a	<0.001	<0.01
1-DP	1.69 ± 0.02	2.60 ± 0.06^c	1.98 ± 0.02^a	2.23 ± 0.03^b	<0.001	<0.001
HMF	0.68 ± 0.02	0.35 ± 0.05^a	0.31 ± 0.03^a	1.15 ± 0.06^b	<0.01	<0.001
Glycation products, μg g^{-1} sample (μg g^{-1} protein)						
Furosine	1298 ± 39 (1670 ± 50)	2499 ± 182^a (3172 ± 231^a)	2187 ± 79^a (2893 ± 105^a)	4662 ± 87^b (6166 ± 115^b)	<0.01	<0.001
CML	74.6 ± 2.0 (96.1 ± 2.6)	144 ± 10^a (182 ± 13^a)	121 ± 3^a (160 ± 4^a)	301 ± 11^b (399 ± 14^b)	<0.01	<0.001
CEL	<LOQ	<LOQ	<LOQ	<LOQ	–	
MG-H	1.58 ± 0.11 (2.03 ± 0.14)	0.82 ± 0.03^a (1.04 ± 0.04^a)	2.06 ± 0.14^b (2.73 ± 0.19^b)	3.20 ± 0.21^c (4.23 ± 0.28^c)	0.014	<0.01
GO-H	<LOQ	<LOQ	<LOQ	<LOQ	–	
GOLD	<LOQ	<LOQ	<LOQ	<LOQ	–	
MOLD	<LOQ	<LOQ	<LOQ	<LOQ	–	
AA-derived cross-links, μg g^{-1} sample, (μg g^{-1} protein)						
LAL	87.7 ± 12.6 (113 ± 16)	47.0 ± 2.0^a (59.7 ± 2.5^a)	48.9 ± 1.9^a (64.7 ± 2.5^a)	115 ± 3^b (152 ± 4^b)	0.089 0.086	<0.001
LAN	12.7 ± 0.4 (16.4 ± 0.5)	18.6 ± 1.9 (23.6 ± 2.4)	13.8 ± 0.5 (18.3 ± 0.7)	13.6 ± 0.2 (17.9 ± 0.3)	0.039 0.043	0.064 0.096

Values are presented as mean ± SEM (n = 2–3 per group). p-value$_1$ denotes the comparison between WPC and SPC. p-value$_2$ denotes the overall difference among the three SPC ingredients and values with different superscript letters are significantly different ($p < 0.05$). AA, amino acid; LOQ, limit of quantification; HT-SPC, extra heat-treated (80 °C, 30 s) skim milk-derived whey protein concentrate; HTS-SPC, extra heat-treated (80 °C, 30 s) and stored (37 °C, 70% relative humidity, 6 weeks) skim milk-derived whey protein concentrate; SPC, skim milk-derived whey protein concentrate; WPC, conventional whey protein concentrate.

α-dicarbonyl compounds (3-DG, 3-DGal, 1-DG, and 3,4-DGE) were abundantly present and increased in concentrations after storage, indicating dehydration of hexoses such as glucose, galactose, and fructose. The HMF mirrored this pattern despite being less prevalent and was similarly measured in higher amounts in HTS-SPC relative to SPC and HT-SPC (both $p < 0.001$). The 3-DGal, 3,4-DGE, and HMF concentrations were higher in WPC than SPC, whereas 3-DG and 1-DG were lower (all $p < 0.01$). A greater abundance of 3-DP and 1-DP was found in SPC compared to WPC (both $p < 0.001$), with levels lowered during storage ($p < 0.01$) and as a consequence of heat treatment (<0.001), respectively. Glyoxal and methylglyoxal, the shorter chain α-dicarbonyl compounds, were also decreased in HTS-SPC compared to SPC and HT-SPC (both $p < 0.01$), and the concentrations were lower in WPC than in SPC (both $p < 0.01$). Neither glucosone nor galactosone, the oxidation products of glucose and galactose, respectively, were detected in the samples. As intermediate compounds of the Maillard reaction, α-dicarbonyl compounds can react with the amino acid residues of proteins and lead to formation of AGEs over time. This was confirmed by the higher levels of CML and lower levels of glyoxal (a precursor of CML) in HTS-SPC compared to SPC and HT-SPC (both $p < 0.001$). Likewise, MG-H levels were two to four times higher in HTS-SPC compared to SPC and HT-SPC (both $p < 0.05$). The higher concentration of furosine (the acid derivative of Amadori compounds formed during hydrolysis of samples prior to analysis) in HTS-SPC relative to SPC and HT-SPC (both $p < 0.001$) further indicates that storage of SPC was the most important parameter for the development of the Maillard reaction in the present study. The concentrations of furosine, CML, and MG-H were all lower in WPC than SPC ($p < 0.05$) while CEL, GO-H, GOLD, and MOLD concentrations were below the quantification levels for all whey protein ingredients. Concentrations of LAL and LAN were generally low, although storage caused a 2.5-fold increase in LAL relative to SPC and HT-SPC (both $p < 0.001$). Although not significantly different, the WPC ingredient tended to have a higher level of LAL than the SPC ingredient ($p = 0.09$). The amount of LAN was higher in SPC compared to the WPC ingredient ($p < 0.05$), this difference was, however, reduced during extra heat treatment and storage (both $p > 0.05$ compared to SPC). The cross-links observed by SDS-PAGE were reducible, and thus likely to be due to disulfide formation, while LAL and LAN are both nonreducible cross-links. This suggests that LAN and LAL were either formed mainly intramolecularly in the proteins or formed in such

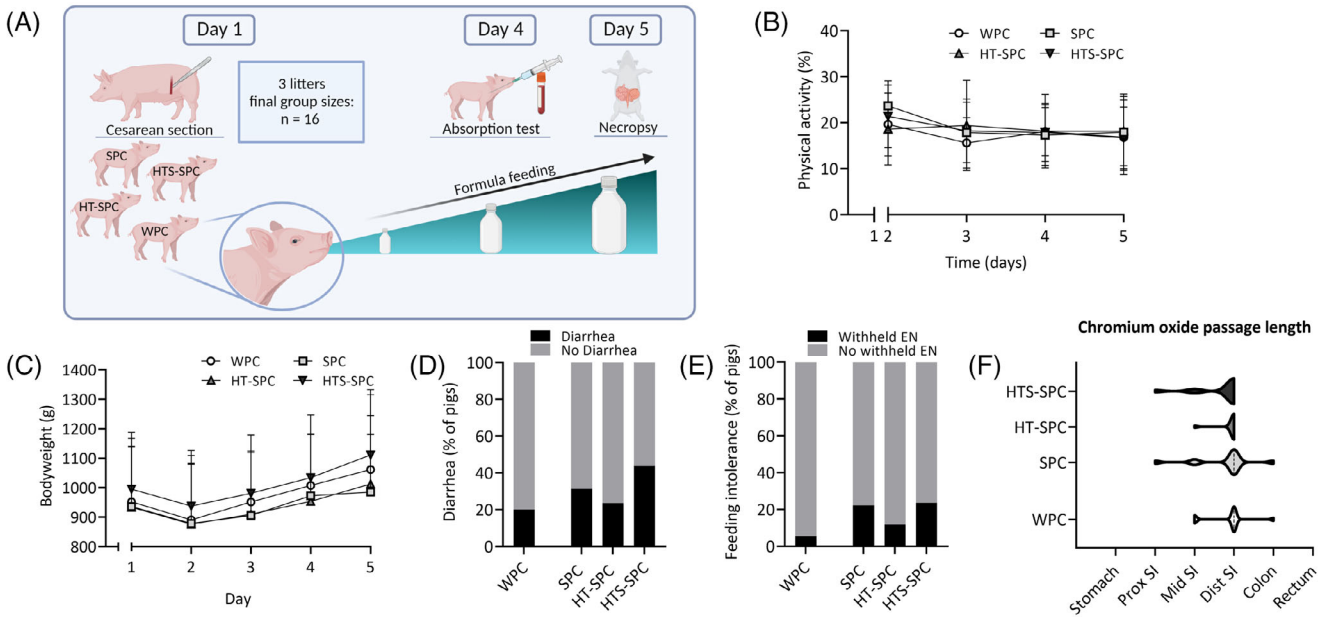

Figure 3. Clinical outcomes and feeding tolerance in preterm piglets fed WPC, SPC, HT-SPC, and HTS-SPC for 5 days. A) In vivo study design, outline created in Biorender.com. B) In-cage physical activity measured as the daily average proportion of active time during an hour. C) Growth curves expressed as the daily body weight. D) Incidence of diarrhea for piglets surviving beyond day 3 (have reached full EN). E) Incidence of feeding intolerance based on withheld EN. F) Passage length of the chromium oxide marker added to the last standardized EN bolus. Continuous data are presented as mean ± SD. For all analyzes: $n = 12–18$ per group. Dist, distal small intestine; EN, enteral nutrition; HT-SPC, extra heat-treated (80 °C, 30 s) skim milk-derived whey protein concentrate; HT-SPC, extra heat-treated (80 °C, 30 s) and stored (37 °C, 70% relative humidity, 6 weeks) skim milk-derived whey protein concentrate; Mid, middle small intestine; Prox, proximal small intestine; SPC, skim milk-derived whey protein concentrate; WPC, conventional whey protein concentrate.

low concentrations that they were not evident by SDS-PAGE analysis.

3.3. Clinical Status and Feeding Tolerance in Formula-Fed Preterm Piglets

Out of the 72 piglets delivered, 10 died early or were euthanized ahead of schedule due to respiratory distress or iatrogenic complications (catheter-related, such as thrombosis or major external bleeding), i.e., for reasons not related to the interventions. Of these, two piglets survived until day 4 and tissues were collected. The remaining eight piglets were excluded from the study, resulting in final group sizes of 16 (8–9:7–8 male:female ratio) for in vivo analyzes (**Figure 3A**). At the daily clinical assessments, most piglets (95.7%) received a low clinical score of 1–2, leaving supportive therapy unneeded. The in-cage physical activity level, measured from day 2 to 5, was stable and similar for all groups throughout the study period (Figure 3B). Further, the four groups had similar growth performances with average daily body-weight gains expressed as g (kg day)$^{-1}$ of 14 ± 9 for WPC, 16 ± 7 for SPC, 15 ± 8 for HT-SPC, and 19 ± 7 for HTS-SPC (Figure 3C). Except for an increased stomach weight and reduced heart weight of SPC relative to WPC pigs (both $p < 0.05$), organ dimensions and blood biochemistry variables including blood urea nitrogen levels (by-product of protein metabolism) were comparable among the groups (Table S4, Supporting Information).

The incidence of diarrhea (Figure 3D) was not differently affected by the dietary interventions and no rectal bleeding was observed. Likewise, the individual enteral feeding plan was only interrupted a few times due to clinical signs of gastrointestinal dysfunction and the incidence of feeding intolerance was similar between groups (Figure 3E). Further, comparable gastrointestinal transit times for the four groups were indicated by similar first passage of meconium in hours postpartum (the median [IQR] was 23 [16–30] for WPC, 22 [11–31] for SPC, 25 [18–32] for HT-SPC, and 21 [14–2] for HTS-SPC), stomach emptying rate (gastric residuals 1 h after receiving the last EN bolus, Table S4, Supporting Information) and passage length of the ingested chromium oxide marker (Figure 3F). Overall, there was little variation in intestinal food passage within groups and in most cases (78.9%) the last enteral bolus reached the distal small intestine after 60 min.

3.4. Gut Inflammation and Development in Formula-Fed Preterm Piglets

Macroscopic NEC (score ≥4) occurred primarily in the stomach and colon (17% and 16%, respectively), with fewer lesions in the small intestine (8%). Across groups, the overall NEC incidence and pathological severity were similarly low (**Figure 4A**). For HT-SPC pigs, the pathological severity of the colon was lower compared with SPC and HTS-SPC pigs (both $p < 0.05$). Microscopically, tissue from animals with and without small intestinal

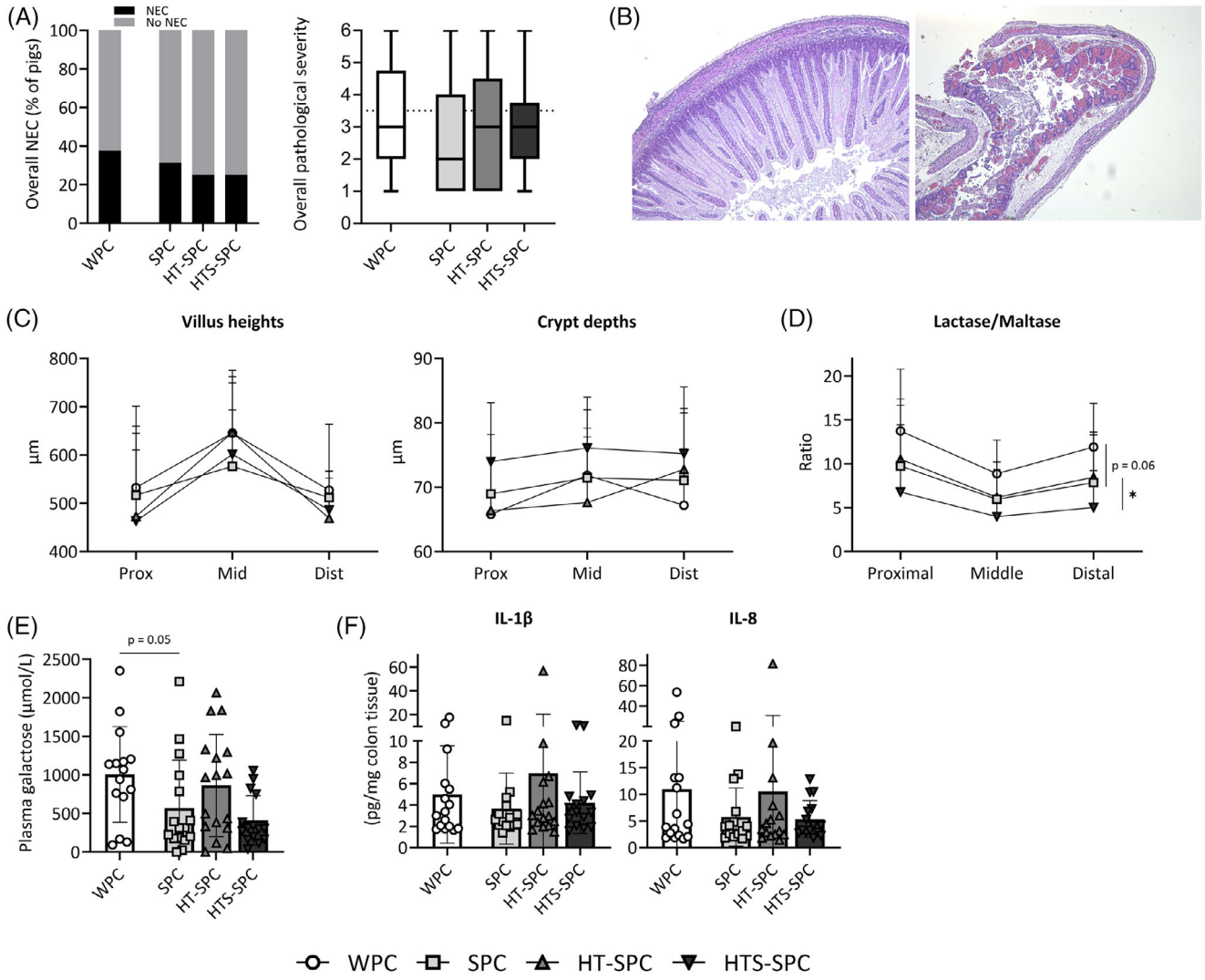

Figure 4. Gut maturation in preterm piglets fed WPC, SPC, HT-SPC and HTS-SPC for 5 days. A) NEC incidence (left panel) and lesion severity (right panel) of the entire gastrointestinal tract. The dotted horizontal line demonstrates the criteria for NEC diagnosis (≥4). B) Representative micrographs (10×) of hematoxylin and eosin-stained transverse sections of intact (left panel) and severely affected small intestine (villi erosion, thickened submucosa and erythrocyte extravasation, right panel). C) Villus heights and crypt depths measured across the small intestine. D) Activity of lactase-to-maltase ratio measured across the small intestine. E) Absorptive capacity expressed as the plasma galactose concentration 20 m after oral administration. F) Colon tissue levels of proinflammatory cytokines. Ordinal data, i.e., NEC scores, are presented as box plots showing the median and IQR. Continuous data are presented as mean ± SD. For all analyzes: n = 10–17 per group. Values not sharing the same letters are significantly different ($p < 0.05$). *, $p < 0.05$. HT-SPC, extra heat-treated (80 °C, 30 s) skim milk-derived whey protein concentrate; HT-SPC, extra heat-treated (80 °C, 30 s) and stored (37 °C, 70% relative humidity, 6 weeks) skim milk-derived whey protein concentrate; SPC, skim milk-derived whey protein concentrate; WPC, conventional whey protein concentrate.

lesions showed distinct histological variations (Figure 4B), which supports the macroscopic evaluation. Only pigs with a macroscopic lesion score of 3 or 4 in the distal small intestine had elevated plasma levels of I-FABP. Consistent with the similar small intestinal NEC scores, we found no group differences in plasma I-FABP levels (Table S5, Supporting Information). Likewise, changes to the small intestinal mucosal architecture were too subtle to differentiate the villus heights and crypt depths between groups (Figure 4C). Brush border enzyme activities measured across the small intestine showed, however, that SPC pigs had a lower lactase level ($p < 0.05$) and a tendency towards a reduced lactase-to-maltase ratio compared to WPC pigs ($p = 0.06$; Figure 4D). Further, SPC pigs tended to have lower plasma galactose levels than WPC pigs ($p = 0.05$; Figure 4E), suggesting that their intestinal absorption capacity was mildly reduced. Between the SPC-fed groups, HTS-SPC increased maltase activity (relative to SPC, $p < 0.05$) and tended to decrease lactase activity (relative to HT-SPC, $p = 0.05$) across the small intestine of preterm pigs, resulting in a reduced lactase-to-maltase ratio (relative to HT-SPC, $p < 0.05$; Figure 4D). Additionally, the activity of aminopeptidase N was elevated in the distal small intestine among HTS-SPC pigs compared with SPC pigs ($p < 0.05$; Table S5, Supporting Information). All parameters of gut structure and function are listed in Table S5, Supporting Information. To further investigate

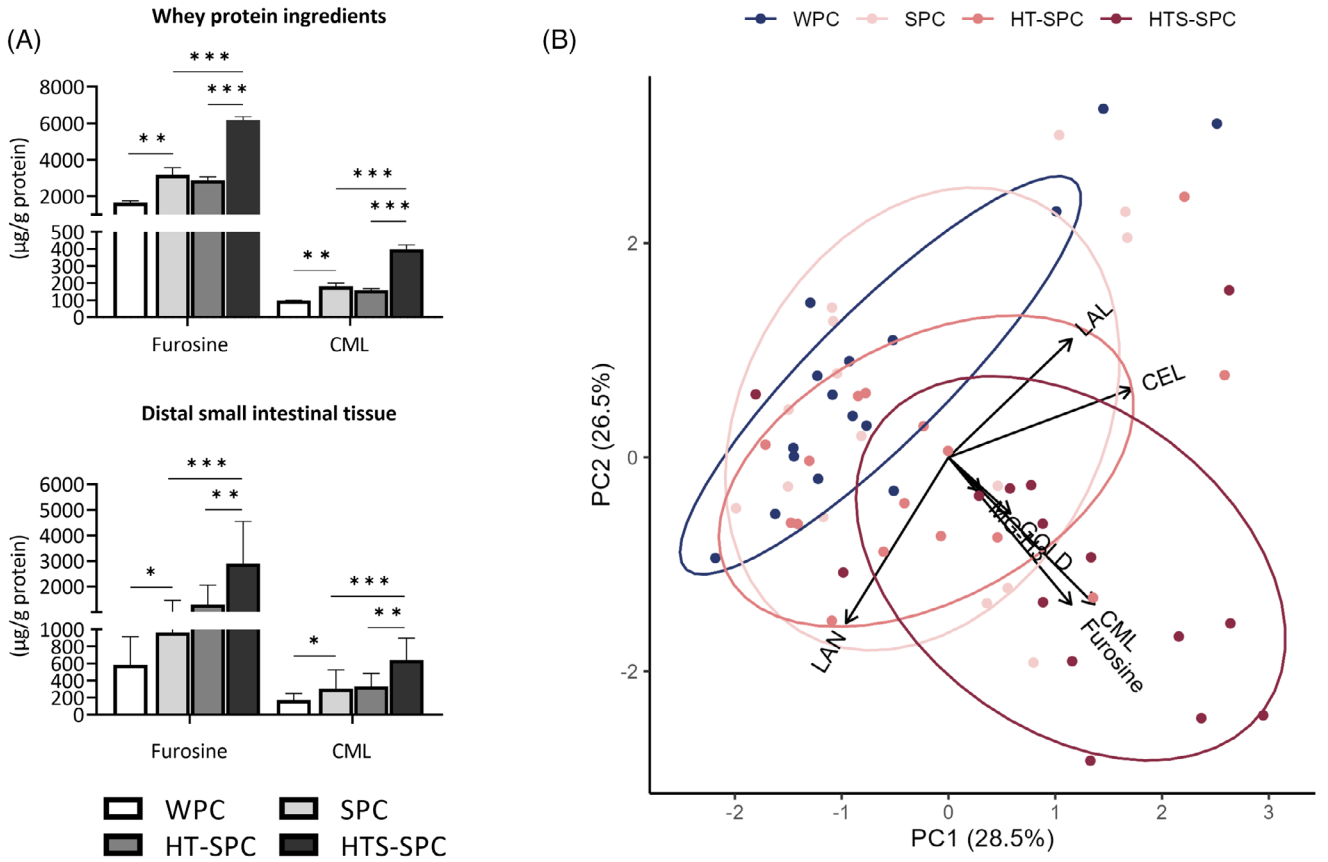

Figure 5. MRPs and amino acid cross-links in distal small intestinal tissue from preterm piglets fed WPC, SPC, HT-SPC, and HTS-SPC for 5 days. A) Furosine and CML measured in whey protein ingredients (top panel) and distal small intestinal tissue from associated pigs (bottom panel). Data are presented as mean ± SD. B) PCA biplot based on MRPs and amino acid cross-links in distal small intestinal tissue. Furosine, CML, CEL, MG-H, GOLD, LAL, and LAN were included as loading vectors. For ingredients data: $n = 2$–3 per group. For pig data: $n = 15$–16 per group. *, $p < 0.05$; **, $p < 0.01$;***, $p < 0.001$. HT-SPC, extra heat-treated (80 °C, 30 s) skim milk-derived whey protein concentrate; HT-SPC, extra heat-treated (80 °C, 30 s) and stored (37 °C, 70% relative humidity, 6 weeks) skim milk-derived whey protein concentrate; SPC, skim milk-derived whey protein concentrate; WPC, conventional whey protein concentrate.

the observed group differences in colon lesion severity between SPC-fed groups, the levels of proinflammatory cytokines (TNF-α, IL-1β, and IL-8) were evaluated in resected tissue (Figure 4F). Similar levels of IL-1β and IL-8 were measured in all groups, while TNF-α were below the detection limit in 84% of the samples.

3.5. Effects of Dietary MRP Accumulation in the Gut

MRPs and amino acid cross-links were measured in distal small intestinal tissue. Furosine, CML, CEL, MG-H, GOLD, LAL, and LAN were all detected, whereas GO-H and MOLD levels were below the limit of quantification (Table S6, Supporting Information). As for the whey protein ingredients, furosine and CML were the two most abundant MRPs identified in the tissue samples, and both were detected in lower amounts in WPC pigs relative to SPC pigs (both $p < 0.05$, **Figure** 5A). Between SPC-fed groups, HTS-SPC pigs had two to three times higher levels of both furosine and CML (Figure 5A) in the distal small intestine (all $p < 0.01$), corresponding to the higher levels measured in the ingredient (all $p < 0.001$). The principal component analysis (PCA) biplot confirms that the positively correlated furosine and CML concentrations are indeed the two determining variables in differentiating the HTS-SPC pigs from the remaining three groups (Figure 5B). If only furosine and CML are included in the PCA plot, the PC1 increases to 84.7% explained variation as opposed to 28.5% when all identified MRPs and amino acid cross-links are considered. In agreement with the low-grade small intestinal inflammation observed across all groups, qPCR revealed only minor fold changes in a few selected differently expressed genes (Table S7, Supporting Information). Despite this, the expression of *TNFAIP3*, which is rapidly induced by the proinflammatory cytokine TNF, was upregulated in HTS-SPC pigs compared to HT-SPC pigs ($p < 0.05$). In turn, HT-SPC pigs had a higher expression of *CASP1* relative to SPC pigs ($p < 0.05$). Additionally, genes involved in the inhibition of apoptosis (*PIK3C3* and *PIKFYVE*) were suppressed in HTS-SPC compared to HT-SPC pigs (both $p < 0.05$). Genes encoding proteins related to oxidative stress (*OXR1*), regulation of inflammatory responses

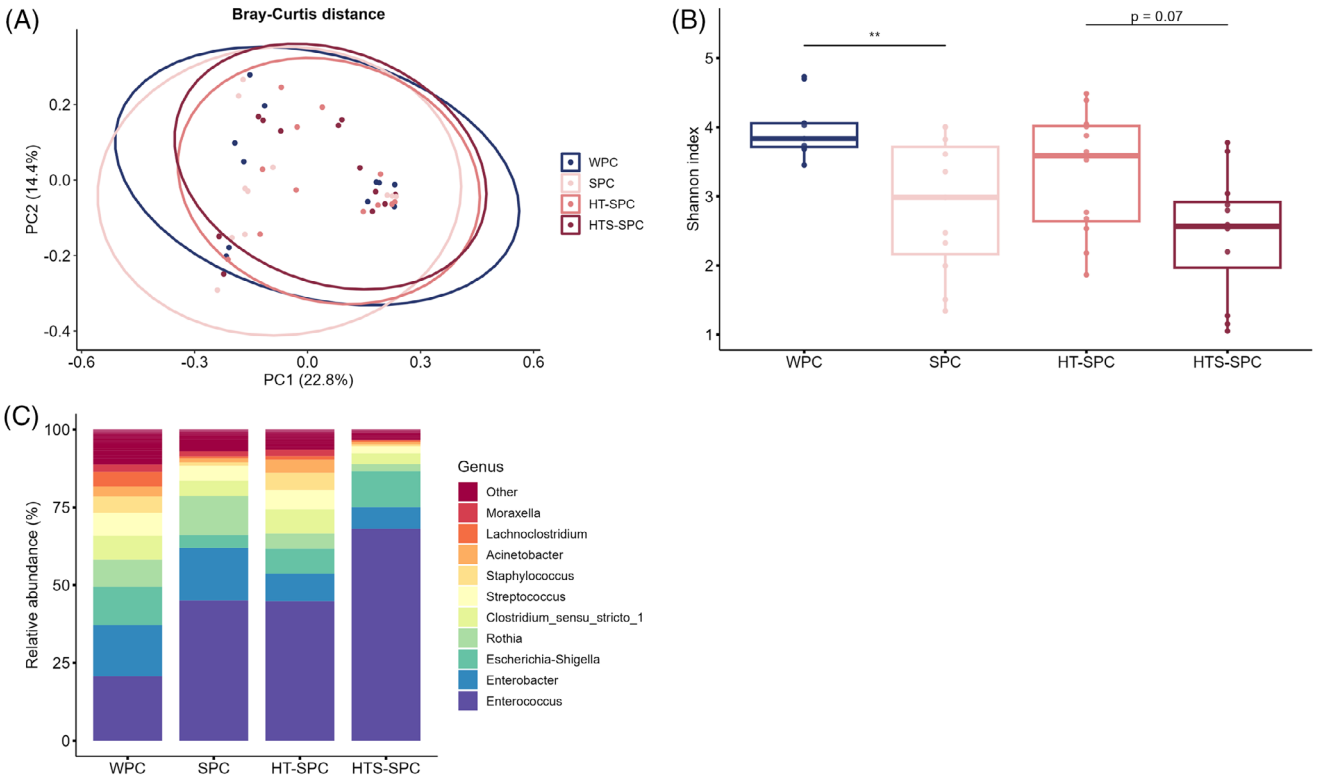

Figure 6. Colonic bacterial composition of preterm piglets fed WPC, SPC, HT-SPC, and HTS-SPC for 5 days. A) PCA plot depicting beta diversity based on the Bray–Curtis dissimilarity measure (unweighted distance metric). B) Boxplot visualizing the Shannon index as a measure of alpha diversity. C) Relative bacterial abundance averaged at genus level. For all analyzes: n = 12–15 per group. **, $p < 0.01$. HT-SPC, extra heat-treated (80 °C, 30 s) skim milk-derived whey protein concentrate; HT-SPC, extra heat-treated (80 °C, 30 s) and stored (37 °C, 70% relative humidity, 6 weeks) skim milk-derived whey protein concentrate; SPC, skim milk-derived whey protein concentrate; WPC, conventional whey protein concentrate.

(*NFKB1* and *VCAM1*) and gut integrity (*TJP1*) were all downregulated in SPC compared to WPC pigs (all $p < 0.05$).

3.6. Gut Microbial Composition in Formula-Fed Preterm Piglets

The four groups had a similar colonic bacterial composition (**Figure 6**A). The Shannon index revealed a lower alpha diversity in SPC, relative to WPC pigs ($p < 0.01$), while a tendency towards a decreased bacterial diversity was observed for HTS-SPC compared to HT-SPC pigs ($p = 0.07$; Figure 6B). Across the groups, *Enterococcus* was the predominant genus (Figure 6C) although less abundant in colon content from WPC relative to SPC pigs (Figure S1A, Supporting Information). As a result, there was a greater evenness in the relative abundance of major genera constituting the gut microbiome of WPC pigs. Notably, the relative abundance of *Escherichia/Shigella* differed between the SPC-fed groups; however, overall, differential relative abundances were seen in few low-abundant genera (Figure S1B, Supporting Information).

3.7. Systemic Immune Development in Formula-Fed Preterm Piglets

Overall, the incidence of bone marrow infections was relatively high, with 64% for WPC, 57% for SPC, 63% for HT-SPC, and 83% for HTS-SPC (**Figure 7**A). Neither the infection density nor the incidence of bacterial infections in the bone marrow could be clearly distinguished between groups. All hematological and systemic immune parameters are listed in Table S8, Supporting Information. SPC pigs had slightly higher red blood cell counts, hemoglobin, and hematocrit values compared to WPC pigs (all $p < 0.05$) and a lower platelet count relative to HT-SPC pigs ($p < 0.01$), none of which is explained by clinical or paraclinical findings. All groups had a similar neutrophil phagocytic rate and activity, implying that their innate immune response capacity was comparable. The circulating neutrophil count in HTS-SPC pigs was, however, decreased compared to HT-SPC pigs ($p < 0.05$, Figure 7B), which could be due to neutrophils leaving the bloodstream to infiltrate inflamed tissue. Similarly, the increased TNF-α response observed following bacterial stimulation was driven by HTS-SPC pigs with macroscopic NEC (Figure 7C). A lower frequency of cytotoxic T cells in HTS-SPC relative to HT-SPC pigs ($p < 0.05$, Figure 7D) resulted in a tendency towards an increased CD4/CD8 T-cell ratio ($p < 0.1$). Finally, relative to SPC pigs, we estimated a lower T-cell frequency of WPC pigs ($p < 0.01$, Figure 7D).

4. Discussion

Optimizing IFs to improve the development of formula-fed infants remains crucial, particularly for those born preterm who

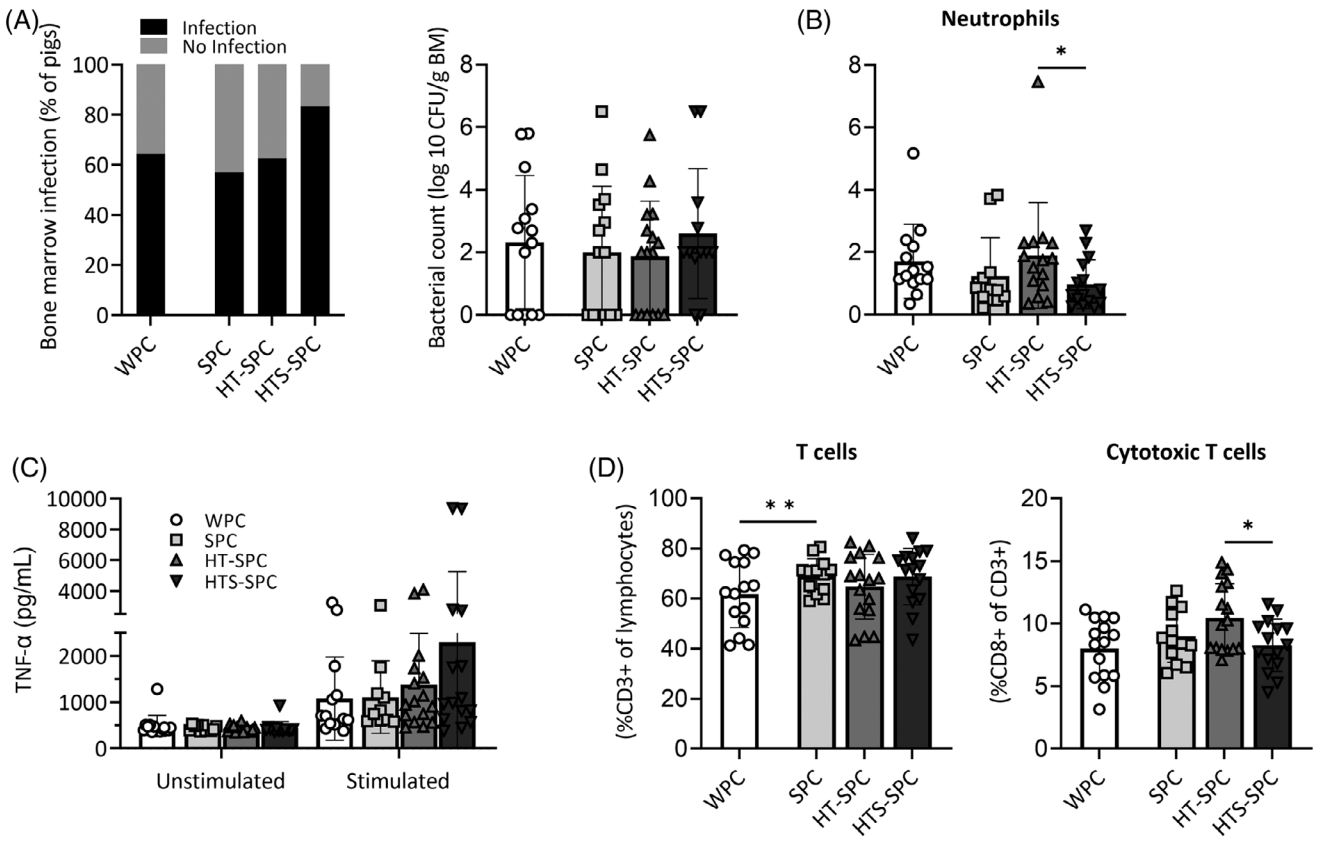

Figure 7. Blood cell counts and systemic immune function in preterm piglets fed WPC, SPC, HT-SPC, and HTS-SPC for 5 days. A) Incidence of infection (left panel) and quantitation of bacteria in bone marrow (right panel). B) Blood neutrophil counts. C) TNF-α levels in blood samples before and after a stimulation with *S. epidermidis*. D) Frequency of T cells (CD3+ lymphocytes, left panel) and cytotoxic T cells (CD3+CD4-CD8+, right panel). Continuous data are presented as mean ± SD. For all analyzes: $n = 11$–16 per group. *, $p < 0.05$; **, $p < 0.01$. BM, bone marrow; HT-SPC, extra heat-treated (80 °C, 30 s) skim milk-derived whey protein concentrate; HT-SPC, extra heat-treated (80 °C, 30 s) and stored (37 °C, 70% relative humidity, 6 weeks) skim milk-derived whey protein concentrate; SPC, skim milk-derived whey protein concentrate; WPC, conventional whey protein concentrate.

are highly sensitive to the dietary feeding protocol due to an immature gut and immune system at birth.[54–57] Using a preterm pig model, we assessed the gastrointestinal and immunological responses to IFs containing differently processed whey protein ingredients.

In the current study, feeding differently processed whey protein ingredients did not affect clinical parameters such as mortality, clinical score, weight gain, physical activity, and organ weights. All whey protein ingredients were similarly tolerated, as demonstrated by the small variation in intestinal food passage between pigs and low group incidences of feeding intolerance and diarrhea. Levels of blood urea nitrogen, a marker of in vivo protein load, and creatinine, viewed as a proxy measure of kidney function, were independent of the dietary intervention and within normal range for nursing piglets,[58] strengthening the preclinical safety of the SPC ingredient. Still, the clinical profile and effects on gut maturation in direct comparison to an optimal raw milk diet[26,50] is unknown and a weakness in this study design.

The methods employed for isolating whey proteins affect the proteins' structural and functional properties.[28] Here, the SPC ingredient was produced directly from pasteurized bovine skim milk using microfiltration, whereas the conventional WPC is obtained as a by-product from cheese manufacturing. Due to the different stream flows, compositional differences are inevitable, and as such, the greater quantities of α-lactalbumin and β-lactoglobulin in SPC and the absence of casein glycomacropeptide relative to WPC[31] likely explain the differences observed in amino acid profiles. Characterization of the SPC ingredients revealed structural protein modifications after heat treatment and storage. During heating, denatured protein molecules are available for aggregate formation.[59] In the current study, SDS-PAGE revealed the presence of large disulfide-linked protein aggregates in the WPC and heat-treated and stored SPC ingredients, while the minimally processed SPC did not contain any notable amounts of aggregates. Previously, the involvement of important bioactive proteins such as LF in heat-induced protein aggregates has been demonstrated.[12] This may explain the discrepancy between the total amount of LF measured by LC-MS (highest in the WPC ingredient) and nonaggregated LF measured by ELISA[60] (highest in SPC) in the present study. In accordance with previous in vitro studies,[61,62] heat treatment of SPC resulted in a decreased abundance of native LF, verifying its heat labile nature. Overall, the native LF amounts, reaching ≈135 μg mL^{-1} in the SPC formula diet, are considerably below the levels measured in bovine colostrum (1–2 mg mL^{-1}[7]) and

sow milk (≈3 mg mL^{-1}[63]), illustrating one of the issues associated with feeding processed infant formula as opposed to a raw milk diet.

Despite variations in native LF levels, WPC and SPC both exerted in vitro growth inhibition of *S. epidermidis* (6 h), thus indicating a similar bioactive potential, extending beyond the effects of LF. Additional heat treatment led to a minor reduction in the bacteriostatic potential of SPC, confirming the negative correlation between heat intensity and antibacterial capacity of bovine whey proteins, such as LF, lactoperoxidase, and immunoglobulins.[64,65] In the current study, *E. faecalis* eluded the antibacterial effects of all whey protein ingredients. The reduced bacterial inhibitory effect of WPC compared to SPC could be explained by lower levels of native whey proteins, including LF, albeit the higher fat content in WPC may have had an impact given the lipolytic ability of *E. faecalis*.[66,67]

Besides affecting the tertiary structure of proteins, heat treatment and storage also favors chemical modifications through the Maillard reaction.[17,19] Increased concentrations of furosine, CML, and MG-H in HTS-SPC compared to SPC and HT-SPC support our earlier findings emphasizing the impact of storage on the progression of Maillard reactions.[24] This was further supported by lower levels of AGE precursors (glyoxal and methylglyoxal), increased color formation and increasing levels of six-carbon α-dicarbonyl compounds in the HTS-SPC ingredient. Based on the repeated heat treatments during production of WPC, we were surprised to find a lower level of glycation compounds compared to SPC. However, the SPC ingredient contains more lactose than WPC, which is essential for the formation of glycation compounds.[17] The lower level of glycation compounds in WPC is therefore most likely due to the lower lactose:protein ratio compared to SPC.

The overall low NEC incidence in this study, may be explained by the deliberate omission of maltodextrin in the diet, a precautionary measure to ensure that any detrimental effects of the whey protein ingredients, including the different levels of glycation products, were not confounded by the NEC-inducing effects of maltodextrin.[50] Similar to the present study, we recently observed that preterm piglets fed an ultra-high temperature-treated IF with a high content of glycation products showed signs of gut dysfunction and inflammation despite an overall low NEC incidence.[24] Dietary AGEs constitute a structurally heterogeneous group, which results in a wide range of in vivo metabolic profiles and tissue distribution patterns.[67] In a mouse model, the ileum was previously identified as a major site of protein-bound labeled CML accumulation upon long-term dietary exposure.[68] Accordingly, the difference in furosine and CML levels between the whey protein ingredients was reflected in the ileal tissue accumulation in the pigs. Together with the PCA biplot, this finding indicates that the difference in tissue MRP levels between groups was mainly attributed to the diets. The CEL and GOLD were though only detected in the intestinal tissue and not identified in the protein ingredients, suggesting an endogenous formation of these compounds and underlining the difficulty in determining the direct physiological implications of exogenous glycation products.[69]

AGEs can exert detrimental biological effects either directly by protein cross-linking and structural deformation or indirectly by receptor-mediated activation of downstream inflammatory pathways.[70,71] RAGE, a member of the immunoglobulin superfamily of receptors,[70] is expressed by intestinal epithelial cells especially during inflammation[72] and distributed throughout the intestinal tract.[23] As such, a knockout mouse-model have shown that CML-modified proteins, isolated from biopsies of patients with inflammatory bowel disease, were able to elicit a RAGE-dependent intestinal inflammatory response after rectal application.[21] Here, signs of small intestinal mucosal injury were observed among HTS-SPC pigs, as a rapid postnatal decrease in the lactase-to-maltase ratio compared to HT-SPC pigs, suggests tissue damage and subsequent regeneration of the epithelium.[73] The upregulation of *TNFAIP3* in the distal small intestine of HTS-SPC pigs, compared to HT-SPC pigs, confirms a recent TNF-induced inflammatory response (*TNF* upregulated 2.3 times in HTS-SPC relative to HT-SPC, $p = 0.07$; Table S7, Supporting Information). *PIK3C3* and *PIKFYVE*, two genes related to the antiapoptotic phosphatidylinositol-3-kinase/protein kinase B signaling pathway,[74] were downregulated in HTS-SPC tissue, and this may have enhanced the TNF-mediated cytotoxicity in these pigs. An ongoing intestinal inflammation is likely also responsible for the lower neutrophil blood level in pigs fed HTS-SPC compared to HT-SPC, and this neutrophil migration across the intestinal epithelium may have been mediated by RAGE.[72] Correspondingly, the MRP-induced gut inflammation observed in HTS-SPC pigs may be responsible for cytotoxic T cells homing to the gut,[75] causing a temporary drop in the blood levels compared to HT-SPC pigs.

In line with the higher intake of dietary MRP levels, SPC-fed pigs displayed some signs of intestinal mucosal injury, such as a lower lactase level and a tendency to a reduced absorptive capacity relative to WPC pigs. In contrary, gene expression analysis revealed elevated levels of genes related to oxidative stress and inflammation (*OXR1*, *NFKB1*, and *VCAM1*) in WPC, compared to SPC pigs. The expression of VCAM1, a proinflammatory adhesion molecule upregulated in the gut of patients with inflammatory bowel disease and in various experimental models of colitis,[76] has proved to be both RAGE-[77,78] and NFKB-dependent,[79] which advocates induction of the AGE-RAGE signaling pathway. It may be speculated that the lower level of MRPs in the WPC ingredient resulted in a delayed inflammatory response in the gut possibly reflecting an increased tissue accumulation throughout the study. Conversely, we do not know if the gene expression profile in SPC pigs is an adaptive response to the inflammatory state. Whether this can also explain the decreased level of circulating T cells measured in WPC compared to SPC pigs and the impact of this on the developing immune system, warrants further studies.

A strong correlation has previously been established between the dietary intake of CML and its fecal excretion,[80] thus supporting the notion that unabsorbed AGEs are available for metabolism by the colonic microbiome.[81,82] In juvenile pigs with intrauterine growth restriction, formula-derived MRPs were linked to a reduced gut bacterial diversity and altered bacterial composition.[83] Here, SPC and HTS-SPC decreased the colonic bacterial diversity, as shown by a lower Shannon index, than WPC and HT-SPC, respectively. These differences correlate to the observed glycation products in the ingredients. The preterm gut microbiome is characterized by a facultative dysbiosis often caused by a prolonged dominance of *Enterobacteriaceae* and

Enterococcaceae[84–86] including the genera *Enterococcus*, which was found to be especially abundant in HTS-SPC pigs. As such, a high consumption of MRPs may further delay the colonization of commensal obligate anaerobic bacteria and thereby increase the risk of potential pathogens crossing the intestinal wall.

In summary, the SPC ingredient, with a high level of native proteins, but also slightly higher MRP levels, was tolerated similarly to a conventional WPC-based IF in diet-sensitive preterm pigs used as a model of preterm infants, although minor implications for gut development were observed. Heat treatment and subsequent long-term storage of SPC at suboptimal warm and humid conditions facilitated more protein modifications and MRP formation leading to MRP tissue accumulation and impaired gut maturation and function. The results underline the challenge of retaining native protein structure and the necessity of avoiding formation of chemical protein modifications during processing in order to secure optimal development of sensitive neonates. More studies are needed to document the effects of gently processed whey protein ingredients in IF and dietary MRPs beyond the immediate neonatal period.

Supporting Information

Supporting Information is available from the Wiley Online Library or from the author.

Acknowledgements

The authors acknowledge Nicole Lind Henriksen, Jane Connie Povlsen, and Britta Karlsson from the Section for Comparative Pediatrics and Nutrition at the University of Copenhagen for their involvement in the animal experimental work. The authors thank Karin Tarp and Betina Lyngfeldt Henriksen from the Section for Protein Science and Biotherapeutics at the Technical University of Denmark for their support in running qPCR analyzes. From the Department of Food Science at the University of Copenhagen, they recognize the help of Bente P. Danielsen and Stine Lindskov Gaarde in the sample preparation for the tissue analysis of glycation products and Dennis Sandris Nielsen in supporting the microbiota analysis. Casper Asferg Pedersen (Arla Foods Ingredients Group P/S) is thanked for production of protein ingredient samples. Finally, they appreciate Dereck Edward Chatterton's contribution to the data interpretation. This study was supported by the Ministry of Food, Agriculture and Fisheries of Denmark under the Green Development and Demonstration Program (34009-17-1278) and Arla Foods Ingredients Group P/S (Viby J, Denmark).

Conflict of Interest

A.Bj. and M.R.B. are employed at Arla Foods Ingredients Group P/S. M.N.L., T.T., P.T.S., and S.B.B. have received funding from Arla Foods Ingredients Group P/S. The remaining authors have no conflicts of interest to declare.

Author Contributions

K.A.-O., H.G.A., A.Bj., M.R.B., M.N.L., T.T., P.T.S., and S.B.B. conceptualized and designed the study. K.A.-O., H.G.A., L.I.C., K.E.-K., A.Br., and D.V.S. conducted the animal experiment and laboratory analysis. K.S. advised during the Fluidigm qPCR analysis. K.A.-O., H.G.A., L.I.C., K.E.-K., A.Br., K.S., M.N.L., T.T., P.T.S., and S.B.B. contributed to data interpretation. K.A.-O., H.G.A., M.N.L., and S.B.B. drafted the original manuscript. M.N.L. and S.B.B. were responsible for funding acquisition and project administration. All authors edited and approved the final manuscript version.

Data Availability Statement

The data that support the findings of this study are available from the corresponding author upon reasonable request.

Keywords

bioactive whey protein, gut maturation, Maillard reaction products, preterm neonates, infant formula

Received: July 4, 2023
Revised: December 15, 2023
Published online: February 22, 2024

[1] B. Lönnerdal, *Am. J. Clin. Nutr.* **2014**, *99*, 712S.
[2] O. Ballard, A. L. Morrow, *Pediatr. Clin. North Am.* **2013**, *60*, 49.
[3] W. H. Johnston, C. Ashley, M. Yeiser, C. L. Harris, S. I. Stolz, J. L. Wampler, A. Wittke, T. R. Cooper, *BMC Pediatr.* **2015**, *15*, 173.
[4] S. Ip, M. Chung, G. Raman, P. Chew, N. Magula, D. DeVine, T. Trikalinos, J. Lau, *Evid. Rep. Technol. Assess. (Full Rep.)* **2007**, *153*, 1.
[5] J. Cortez, K. Makker, D. F. Kraemer, J. Neu, R. Sharma, M. L. Hudak, *J. Perinatol.* **2018**, *38*, 71.
[6] Y. Wada, B. Lönnerdal, *J. Nutr. Biochem.* **2014**, *25*, 503.
[7] D. E. W. Chatterton, D. N. Nguyen, S. B. Bering, P. T. Sangild, *Int. J. Biochem. Cell Biol.* **2013**, *45*, 1730.
[8] L. Liu, R. Jiang, B. Lönnerdal, *J. Nutr. Biochem.* **2019**, *69*, 10.
[9] T. Brick, M. Ege, S. Boeren, A. Böck, E. Von Mutius, J. Vervoort, K. Hettinga, *Nutrients* **2017**, *9*, 963.
[10] M. Van Gysel, V. Cossey, S. Fieuws, A. Schuermans, *Eur. J. Pediatr.* **2012**, *171*, 1231.
[11] Y. Liao, R. Alvarado, B. Phinney, B. Lönnerdal, *J. Proteome Res.* **2011**, *10*, 1746.
[12] D. N. Nguyen, P. T. Sangild, Y. Li, S. B. Bering, D. E. W. Chatterton, *J. Dairy Sci.* **2016**, *99*, 959.
[13] Y. Li, D. N. Nguyen, K. Obelitz-Ryom, A. D. Andersen, T. Thymann, D. E. W. Chatterton, S. Purup, A. B. Heckmann, S. B. Bering, P. T. Sangild, *J. Pediatr. Gastroenterol. Nutr.* **2018**, *66*, 128.
[14] G. A. A. van Lieshout, T. T. Lambers, M. C. E. Bragt, K. A. Hettinga, *Crit. Rev. Food Sci. Nutr.* **2019**, *60*, 2422.
[15] Y. Wada, B. Lönnerdal, *J. Agric. Food Chem.* **2014**, *62*, 4175.
[16] Y. Liu, W. Zhang, B. Han, L. Zhang, P. Zhou, *Food Chem.* **2020**, *314*, 126177.
[17] M. Pischetsrieder, T. Henle, *Amino Acids* **2012**, *42*, 1111.
[18] D. Scheidegger, P. M. Radici, V. A. Vergara-Roig, N. S. Bosio, S. F. Pesce, *J. Dairy Sci.* **2013**, *96*, 3414.
[19] S. Milkovska-Stamenova, R. Hoffmann, *Food Chem.* **2017**, *221*, 489.
[20] Y. Joubran, A. Moscovici, R. Portmann, U. Lesmes, *Food Funct.* **2017**, *8*, 2295.
[21] M. Andrassy, J. Igwe, F. Autschbach, C. Volz, A. Remppis, M. F. Neurath, E. Schleicher, P. M. Humpert, T. Wendt, B. Liliensiek, M. Morcos, S. Schiekofer, K. Thiele, J. Chen, R. Kientsch-Engel, A. M. Schmidt, W. Stremmel, D. M. Stern, H. A. Katus, P. P. Nawroth, A. Bierhaus, *Am. J. Pathol.* **2006**, *169*, 1223.
[22] M. Hillman, B. Weström, K. Aalaei, C. Erlanson-Albertsson, J. Wolinski, L. Lozinska, I. Sjöholm, M. Rayner, M. Landin-Olsson, *Food Chem. Toxicol.* **2019**, *125*, 78.
[23] P. Chen, J. Zhao, H. Gregersen, *Dig. Dis. Sci.* **2012**, *57*, 48.
[24] J. Sun, H. G. Akıllıoğlu, K. Aasmul-Olsen, Y. Ye, P. Lund, X. Zhao, A. Brunse, C. F. Nielsen, D. E. W. Chatterton, P. T. Sangild, M. N. Lund, S. B. Bering, *Mol. Nutr. Food Res.* **2022**, *66*, 2200132.

[25] M. L. Jensen, P. T. Sangild, M. Lykke, M. Schmidt, M. Boye, B. B. Jensen, T. Thymann, *Am. J. Physiol. - Regul. Integr. Comp. Physiol.* **2013**, *305*, R4.
[26] Y. Li, M. V. Østergaard, P. Jiang, D. E. W. Chatterton, T. Thymann, A. S. Kvistgaard, P. T. Sangild, *J. Nutr.* **2013**, *143*, 1934.
[27] S. O. Rasmussen, L. Martin, M. V. Østergaard, S. Rudloff, Y. Li, M. Roggenbuck, S. B. Bering, P. T. Sangild, *Am. J. Physiol. - Gastrointest. Liver Physiol.* **2016**, *311*, G480.
[28] B. G. Carter, N. Cheng, R. Kapoor, G. H. Meletharayil, M. A. Drake, *J. Dairy Sci.* **2021**, *104*, 2465.
[29] Y. Chen, M. Callanan, C. Shanahan, J. Tobin, L. F. Gamon, M. J. Davies, L. Giblin, A. Brodkorb, *Dairy* **2021**, *2*, 515.
[30] W. Grimm, *Drug Dev. Ind. Pharm.* **1998**, *24*, 313.
[31] P. Lund, M. R. Bechshøft, C. A. Ray, M. N. Lund, *J. Agric. Food Chem.* **2022**, *70*, 319.
[32] P. Lund, S. B. Nielsen, C. F. Nielsen, C. A. Ray, M. N. Lund, *Food Chem.* **2021**, *348*, 129145.
[33] G. R. Askari, Z. Emam-Djomeh, S. M. Mousavi, *Dry. Technol.* **2008**, *26*, 1362.
[34] D. Felix da Silva, C. Hirschberg, L. Ahrné, A. B. Hougaard, R. Ipsen, *J. Food Eng.* **2018**, *237*, 215.
[35] R. Li, P. Lund, S. B. Nielsen, M. N. Lund, *Food Hydrocoll.* **2022**, *124*, 107206.
[36] H. G. Akıllıoğlu, M. N. Lund, *Food Chem.* **2022**, *366*, 130601.
[37] C. Vinther Schmidt, K. Olsen, O. G. Mouritsen, *Food Chem.* **2021**, *360*, 128971.
[38] G. Hildebrand, M. M. Poojary, C. O'Donnell, M. N. Lund, M. Garcia-Vaquero, B. K. Tiwari, *J. Appl. Phycol.* **2020**, *32*, 1709.
[39] H. G. Akıllıoğlu, D. E. W. Chatterton, M. N. Lund, *Food Chem.* **2022**, *396*, 133687.
[40] J. Cox, M. Mann, *Nat. Biotechnol.* **2008**, *26*, 1367.
[41] D. N. Nguyen, E. Fuglsang, P. Jiang, M. M. Birck, X. Pan, S. B. S. Kamal, S. E. Pors, P. L. Gammelgaard, D. S. Nielsen, T. Thymann, O. Levy, H. Frøkiær, P. T. Sangild, *Innate Immun.* **2016**, *22*, 51.
[42] O. Bæk, S. Ren, A. Brunse, P. T. Sangild, D. N. Nguyen, *Front. Immunol.* **2020**, *11*, 1808.
[43] D. N. Nguyen, A. J. Currie, S. Ren, S. B. Bering, P. T. Sangild, *J. Funct. Foods* **2019**, *57*, 182.
[44] N. Percie du Sert, V. Hurst, A. Ahluwalia, S. Alam, M. T. Avey, M. Baker, W. J. Browne, A. Clark, I. C. Cuthill, U. Dirnagl, M. Emerson, P. Garner, S. T. Holgate, D. W. Howells, N. A. Karp, S. E. Lazic, K. Lidster, C. J. MacCallum, M. Macleod, E. J. Pearl, O. H. Petersen, F. Rawle, P. Reynolds, K. Rooney, E. S. Sena, S. D. Silberberg, T. Steckler, H. Würbel, *Exp. Physiol.* **2020**, *105*, 1459.
[45] P. T. Sangild, T. Thymann, M. Schmidt, B. Stoll, D. G. Burrin, R. K. Buddington, *J. Anim. Sci.* **2013**, *91*, 4713.
[46] A. D. Andersen, P. T. Sangild, S. L. Munch, E. M. van der Beek, I. B. Renes, C. van Ginneken, G. O. Greisen, T. Thymann, *Am. J. Physiol. - Regul. Integr. Comp. Physiol.* **2016**, *310*, R481.
[47] K. Aasmul-Olsen, N. L. Henriksen, D. N. Nguyen, A. B. Heckmann, T. Thymann, P. T. Sangild, S. B. Bering, *Nutrients* **2021**, *13*, 2675.
[48] M. S. Cilieborg, M. Boye, T. Thymann, B. B. Jensen, P. T. Sangild, *J. Parenter. Enter. Nutr.* **2011**, *35*, 32.
[49] R. L. Shen, T. Thymann, M. V. Østergaard, A. C. F. Støy, Ł. Krych, D. S. Nielsen, C. Lauridsen, B. Hartmann, J. J. Holst, D. G. Burrin, P. T. Sangild, *Am. J. Physiol. - Gastrointest. Liver Physiol.* **2015**, *309*, G310.
[50] Y. Li, M. L. Jensen, D. E. W. Chatterton, B. B. Jensen, T. Thymann, A. S. Kvistgaard, P. T. Sangild, *Am. J. Physiol. - Gastrointest. Liver Physiol.* **2014**, *306*, G81.
[51] F. L. Lüthje, K. Skovgaard, H. E. Jensen, L. K. Jensen, *Lab. Anim.* **2018**, *52*, 630.
[52] A. I. S. Andersen-Civil, L. J. Myhill, N. Büdeyri Gökgöz, M. T. Engström, H. Mejer, L. Zhu, W. E. Zeller, J. P. Salminen, L. Krych, C. Lauridsen, D. S. Nielsen, S. M. Thamsborg, A. R. Williams, *FASEB J.* **2022**, *36*, e22256.
[53] S. Ren, Y. Hui, K. Obelitz-Ryom, A. B. Brandt, W. Kot, D. S. Nielsen, T. Thymann, P. T. Sangild, D. N. Nguyen, *Am. J. Physiol. - Gastrointest. Liver Physiol.* **2018**, *315*, G855.
[54] D. N. Nguyen, P. Jiang, H. Frøkiær, P. M. H. Heegaard, T. Thymann, P. T. Sangild, *Sci. Rep.* **2016**, *6*, 36816.
[55] C. F. Hansen, T. Thymann, A. D. Andersen, J. J. Holst, B. Hartmann, L. Hilsted, L. Langhorn, J. Jelsing, P. T. Sangild, *Am. J. Physiol. - Gastrointest. Liver Physiol.* **2016**, *310*, G550.
[56] M. Quigley, N. Embleton, W. Mcguire, *Cochrane Database Syst. Rev.* **2019**, *7*, CD002971.
[57] S. El Manouni El Hassani, D. J. C. Berkhout, H. J. Niemarkt, S. Mann, W. P. De Boode, V. Cossey, C. V. Hulzebos, A. H. Van Kaam, B. W. Kramer, R. A. Van Lingen, J. B. Van Goudoever, D. C. Vijlbrief, M. M. Van Weissenbruch, M. A. Benninga, N. K. H. De Boer, T. G. J. De Meij, *Neonatology* **2019**, *116*, 42.
[58] A. M. Perri, T. L. O'Sullivan, J. C. S. Harding, R. D. Wood, R. M. Friendship, *Can. Vet. J.* **2017**, *58*, 371.
[59] H. Li, T. Zhao, H. Li, J. Yu, *Front. Nutr.* **2021**, *8*, 714869.
[60] N. Kleber, I. Krause, S. Illgner, J. Hinrichs, *Eur. Food Res. Technol.* **2004**, *219*, 105.
[61] Y. Liu, W. Zhang, L. Zhang, K. Hettinga, P. Zhou, *Lwt* **2020**, *133*, 110101.
[62] M. Navis, L. Schwebel, S. S. Kappel, V. Muncan, P. T. Sangild, E. Abrahamse, L. Aunsholt, T. Thymann, R. M. van Elburg, I. B. Renes, *Nutrients* **2020**, *12*, 3391.
[63] M. Jahan, N. Francis, B. Wang, *J. Dairy Sci.* **2020**, *103*, 7521.
[64] L. Xiong, C. Li, S. Boeren, J. Vervoort, K. Hettinga, *Food Res. Int.* **2020**, *127*, 108688.
[65] D. A. Goulding, J. O'Regan, L. Bovetto, N. M. O'Brien, J. A. O'Mahony, *Int. Dairy J.* **2021**, *119*, 105001.
[66] F. Stehr, M. Kretschmar, C. Kröger, B. Hube, W. Schäfer, *J. Mol. Catal. B Enzym.* **2003**, *22*, 347.
[67] M. T. Furumura, P. M. S. Figueiredo, G. V. Carbonell, A. L. Da Costa Darini, T. Yano, *Brazilian J. Microbiol.* **2006**, *37*, 230.
[68] F. J. Tessier, C. Niquet-Léridon, P. Jacolot, C. Jouquand, M. Genin, A. M. Schmidt, N. Grossin, E. Boulanger, *Mol. Nutr. Food Res.* **2016**, *60*, 2446.
[69] K. C. W. van Dongen, L. Kappetein, I. Miro Estruch, C. Belzer, K. Beekmann, I. M. C. M. Rietjens, *Food Chem. Toxicol.* **2022**, *164*, 112987.
[70] C. Ott, K. Jacobs, E. Haucke, A. Navarrete Santos, T. Grune, A. Simm, *Redox Biol.* **2014**, *2*, 411.
[71] M. W. Poulsen, R. V. Hedegaard, J. M. Andersen, B. de Courten, S. Bügel, J. Nielsen, L. H. Skibsted, L. O. Dragsted, *Food Chem. Toxicol.* **2013**, *60*, 10.
[72] K. Zen, C. X.-J. Chen, Y.-T. Chen, R. Wilton, Y. Liu, *J. Immunol.* **2007**, *178*, 2483.
[73] T. Thymann, H. K. Møller, B. Stoll, A. C. F. Støy, R. K. Buddington, S. B. Bering, B. B. Jensen, O. O. Olutoye, R. H. Siggers, L. Mølbak, P. T. Sangild, D. G. Burrin, *Am. J. Physiol. - Gastrointest. Liver Physiol.* **2009**, *297*, G1115.
[74] O. N. Ozes, L. D. Mayo, J. A. Gustin, S. R. Pfeffer, L. M. Pfeffer, D. B. Donner, *Nature* **1999**, *401*, 82.
[75] M. Navis, V. Muncan, P. T. Sangild, L. M. Willumsen, P. J. Koelink, M. E. Wildenberg, E. Abrahamse, T. Thymann, R. M. V. Elburg, I. B. Renes, *Nutrients* **2020**, *12*, 1125.
[76] J. H. Chidlow, D. Shukla, M. B. Grisham, C. G. Kevil, *Am. J. Physiol. - Gastrointest. Liver Physiol.* G5, **2007**, *293*.
[77] E. Boulanger, M. P. Wautier, J. L. Wautier, B. Boval, Y. Panis, N. Wernert, P. M. Danze, P. Dequiedt, *Kidney Int.* **2002**, *61*, 148.
[78] T. N. Perkins, E. A. Oczypok, P. S. Milutinovic, R. E. Dutz, T. D. Oury, *Allergy Eur. J. Allergy Clin. Immunol.* **2019**, *74*, 89.

[79] M. Snelson, E. Lucut, M. T. Coughlan, *Int. J. Mol. Sci.* **2022**, *23*, 1766.
[80] C. Delgado-Andrade, F. É. J. Tessier, C. Niquet-Leridon, I. Seiquer, M. P. Navarro, *Amino Acids* **2012**, *43*, 595.
[81] M. Snelson, M. T. Coughlan, *Nutrients* **2019**, *11*, 215.
[82] Q. Zhang, Y. Wang, L. Fu, *Compr. Rev. Food Sci. Food Saf.* **2020**, *19*, 2559.
[83] G. Elmhiri, D. Hamoudi, S. Dou, N. Bahi-Jaber, J. Reygnier, T. Larcher, S. Firmin, L. Abdennebi-Najar, *Food Funct.* **2016**, *7*, 2582.
[84] J. G. E. Henderickx, R. D. Zwittink, R. A. Van Lingen, J. Knol, C. Belzer, *Front. Cell. Infect. Microbiol.* **2019**, *9*, 85.
[85] Y. Hui, G. Vestergaard, L. Deng, W. P. Kot, T. Thymann, A. Brunse, D. S. Nielsen, *npj Biofilms Microbiomes* **2022**, *8*, 48.
[86] A. Brunse, S. M. Offersen, J. J. Mosegaard, L. Deng, P. Damborg, D. S. Nielsen, P. T. Sangild, T. Thymann, D. N. Nguyen, *Gut Microbes* **2021**, *13*, e1849997.